Parallel to cancer research: No “universal” cure

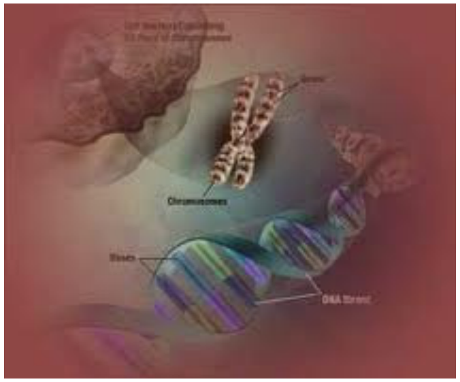

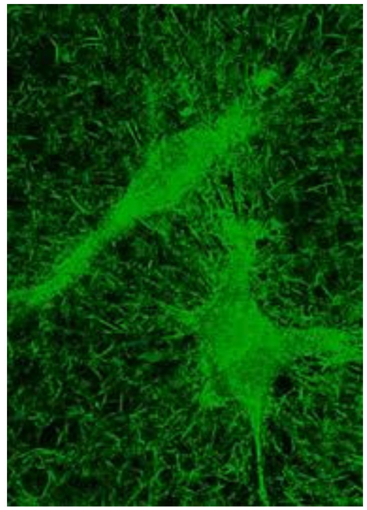

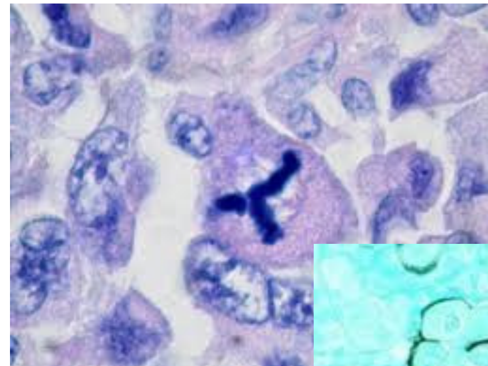

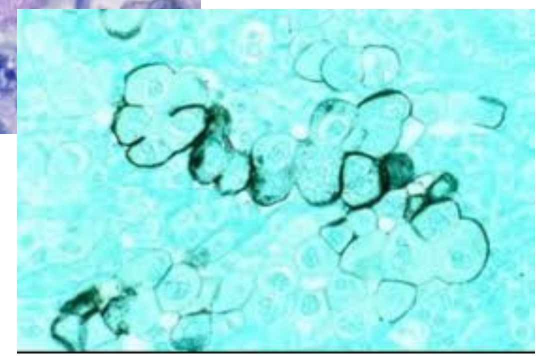

but “management” =

actually helping patients,

tremendous progress made!!

Workshop

"Models versus physical laws/first principles, or why models work?"

Wolfgang Pauli Institute, Vienna, Austria, February 2-5, 2011

"Managing" turbulence ~~theory~~ instead of "curing" turbulence ~~theory~~

and 2 case studies

Charles Meneveau,

Mechanical Engineering & CEAFM,

Johns Hopkins University

JOHNS HOPKINS UNIVERSITY

Mechanical Engineering

Center for Environmental & Applied Fluid Mechanics

Overview of talk:

Two case studies of "managing" the problem -

applying turbulence research all the way to "actual treatment"

- Energy: In the large wind farm of the future, what is the optimal spacing?

Photo appeared in J.N. Sørensen, Annual Rev. Fluid Mech. 2011:

Taken by Uni-Fly A/S
(Wind turbine maintenance company)

- Agriculture: What is the isolation distance to avoid cross-polination?

Motivation : Renewables have low energy density

- solar, wind, wave energy
- need to cover "very, very big" areas
- wind: large wind-farms - on-land & off shore

Land-based HAWT

Shell's Rock River windfarm in Carbon County, Wyoming, USA
Source: http://www.the-eic.com/News/Archive/2005/May/Article503.htm

Horns Rev HAWT
Copyright ELSAM/AS

The windturbine-array boundary layer (WTABL)

From J.N. Sørensen, Annual Rev. Fluid Mech. 2011:

CFD:
Many tools
developed for
detailed simulations

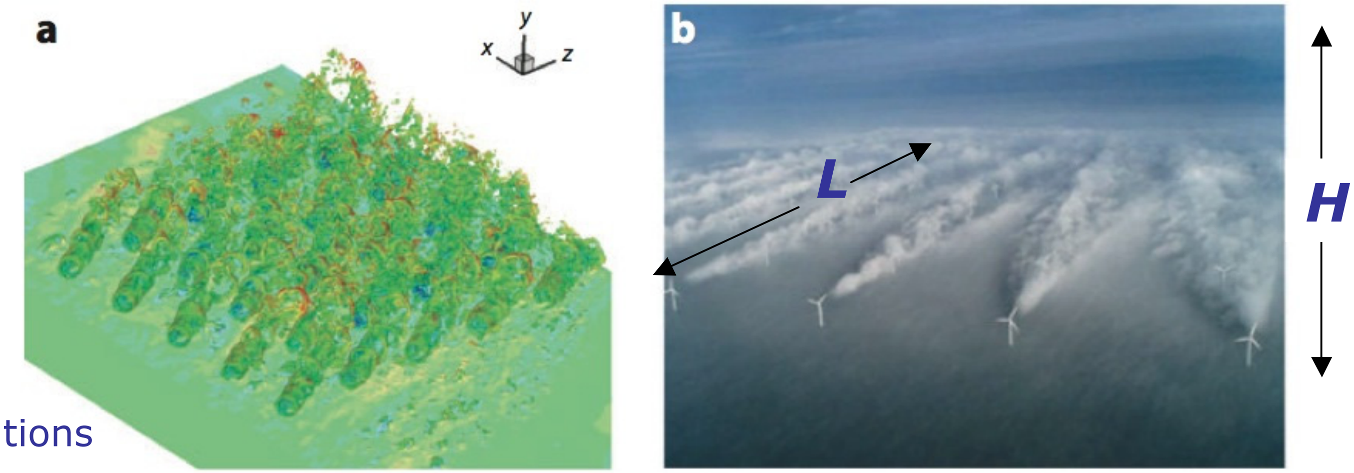

ABL
height

Figure 6

(*a*) Actuator disc computation of a wind farm consisting of 5 × 5 wind turbines. (*b*) Photograph showing the flow field around the Horns Rev wind farm.

Arrays are getting bigger and bigger:

when L > 10 H (H: height of ABL),

approach "fully developed" **FD-WTABL**

What is the most optimal spacing s_{opt} of wind turbines in the fully developed WTABL?

LES: Collaboration with

- Prof. **Johan Meyers** (Univ. Leuven) - LES
- **Marc Calaf** (PhD student EPFL & JHU) + Marc Parlange (EPFL) - LES

Funding: NSF CBET-0730922 (Energy for Sustainability)

Simulations: NCAR allocation (NSF)

Related problem: Wind farm power degradation

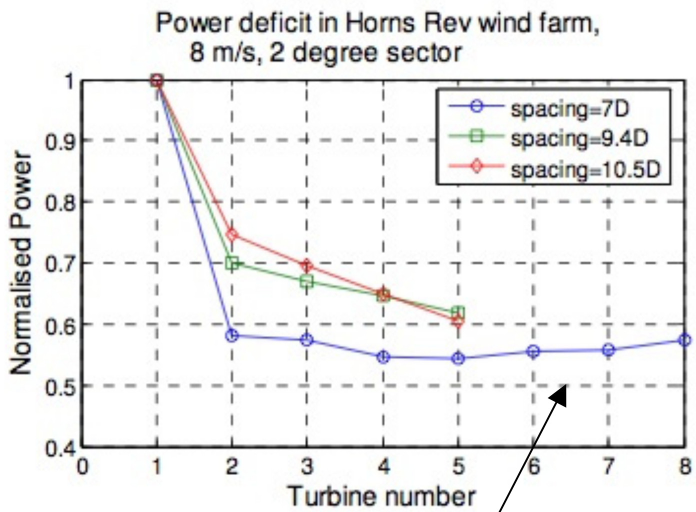

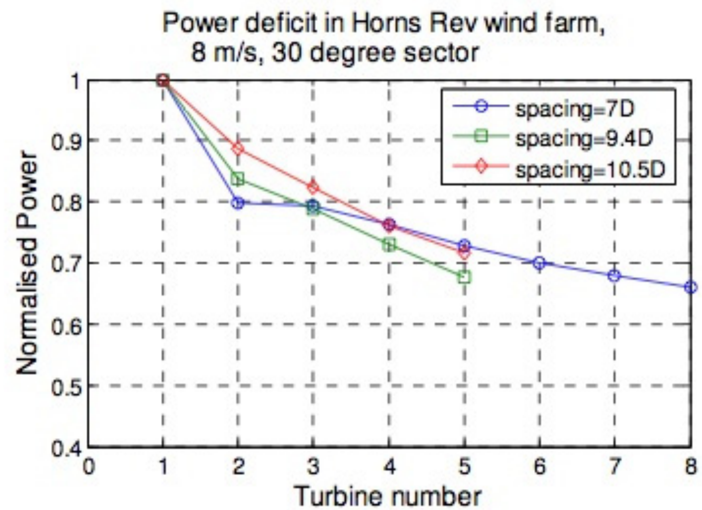

Modelling and measurements of wakes in large wind farms
Barthelemie, Rathmann, Frandsen, Hansen et al…
J. Physics Conf. Series 75 (2007), 012049

- asymptote ??
- how fast?
- is it really around 50%?
- mechanisms ?

The “fully developed” WTABL:

What is the structure of this specific type of boundary layer?

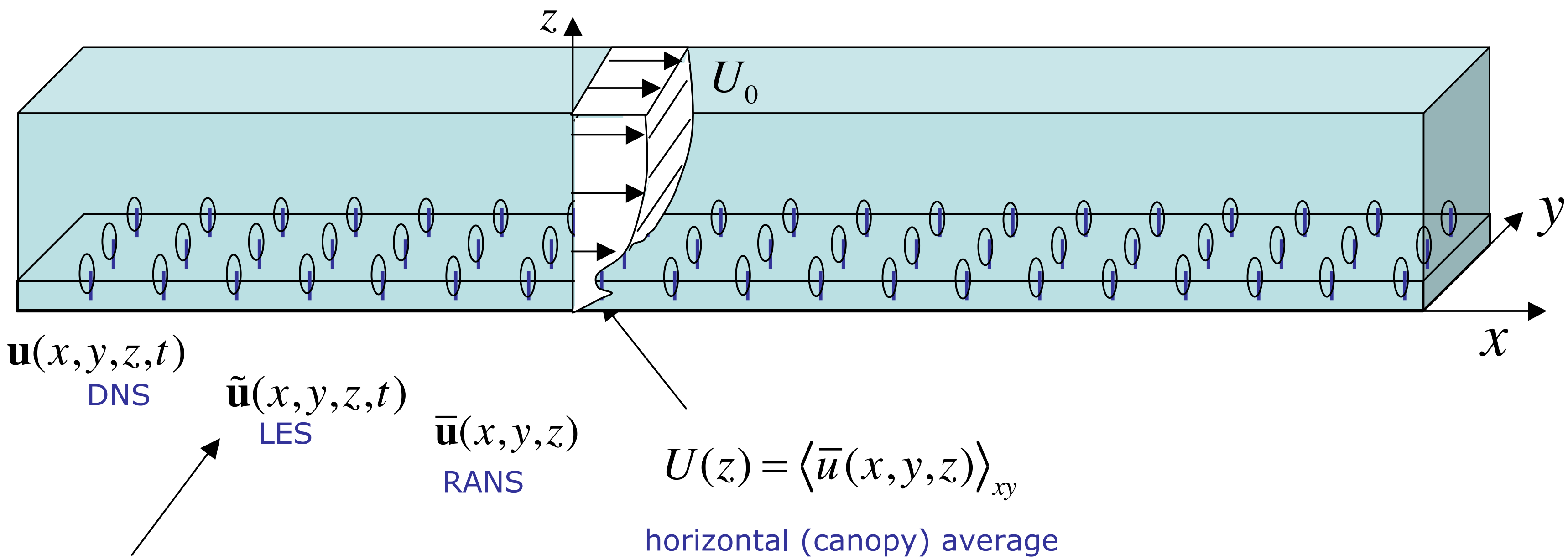

What is the “averaged” velocity distribution? $U(z) = \langle \bar{u}(x,y,z) \rangle_{xy}$

Is there a “universal” WTABL profile?

What are profiles of shear stresses? $\tau_{xz}(z) = -\langle \overline{u'w'} \rangle_{xy}$

Fluxes? TKE flux profiles?

Large Eddy Simulations setup:

- LES code: horizontal pseudo-spectral (periodic B.C.), vertical: centered 2nd order FD (Moeng 1984, Albertson & Parlange 1999, Porté-Agel et al. 2000, Bou-Zeid et al. 2005)

$$H = 1000 - 1500 m, \quad L_x = \pi H - 2\pi H, \quad L_y = \pi H$$
$$(N_x \times N_y \times N_z) = 128 \times 128 \times 128$$

- Horizontal periodic boundary conditions (only good for FD-WTABL)

- Top surface: zero stress, zero w

- Bottom surface B.C.: Zero w + Wall stress: Standard wall function relating wall stress to first grid-point velocity

- Scale-dependent dynamic Lagrangian model

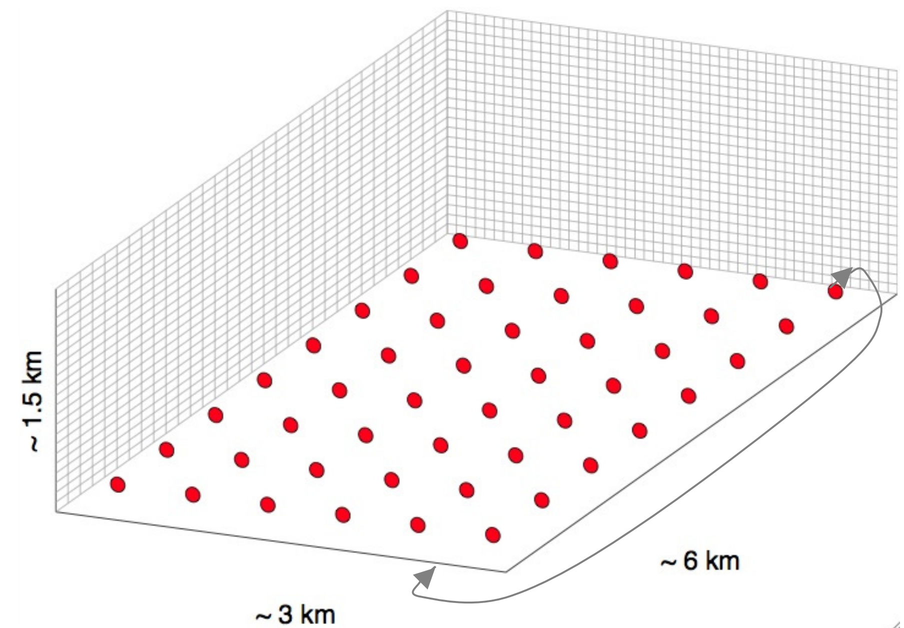

- More details: Calaf, Meneveau & Meyers, “Large eddy simulation study of fully developed wind-turbine array boundary layers” Phys. Fluids. **22** (2010) 015110

Actuator disk modeling of turbines in LES

Jimenez et al., J. Phys. Conf. Ser. **75** (2007) simulated single turbine in LES using dynamic Smag. model

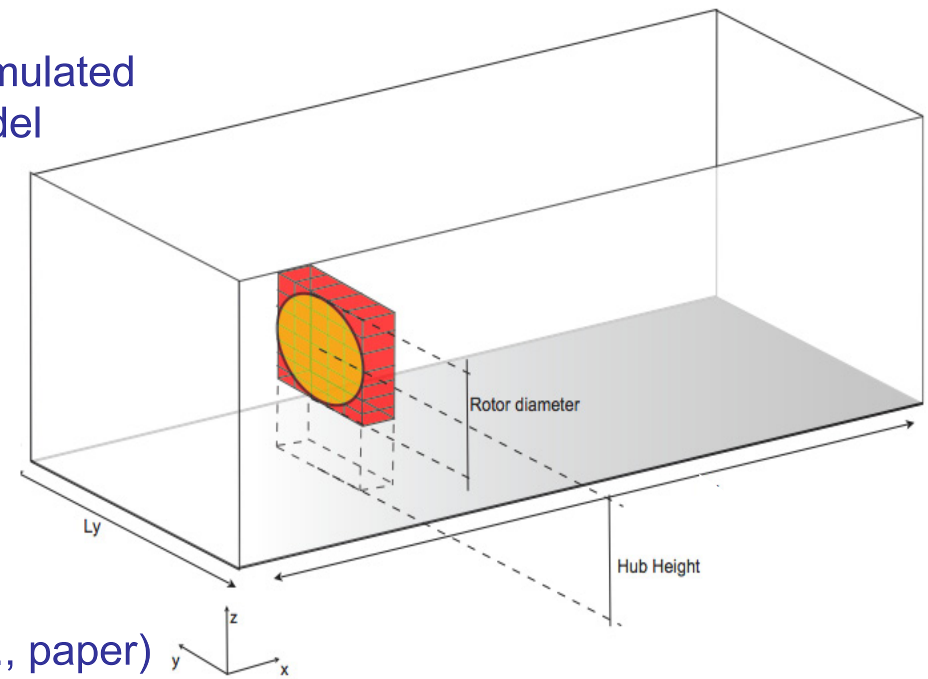

They used fixed reference (undisturbed) velocity:

$$f_{Tx} = -\frac{1}{2} C_T U_{ref}^2 \frac{\delta A_{yz}}{\delta V}, \quad C_T = 0.75$$

Here we use disk-averaged and time-averaged velocity, but local at the disk (see Meyers & Meneveau 2010, 48th AIAA conf., paper)

$$f_{Tx} = -\frac{1}{2} C_T \left(\frac{1}{1-a} \bar{U} \right)^2 \frac{\delta A_{yz}}{\delta V} = -\frac{1}{2} C_T' \bar{U}^2 \frac{\delta A_{yz}}{\delta V}$$

$$C_T = 0.75 \Rightarrow a \approx 0.25 \rightarrow C_T' = 1.33$$

Also, use first-order relax process to time-average:

$$\bar{U}(t) = (1-\varepsilon)\bar{U}(t-dt) + \varepsilon U_{disk}(t)$$

Simulations results:

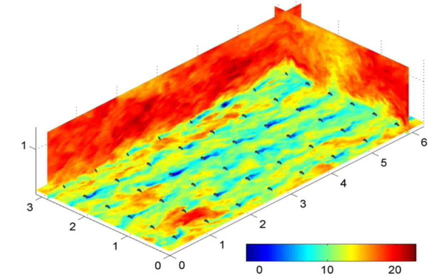

Instantaneous stream-wise velocity contours:

side-view

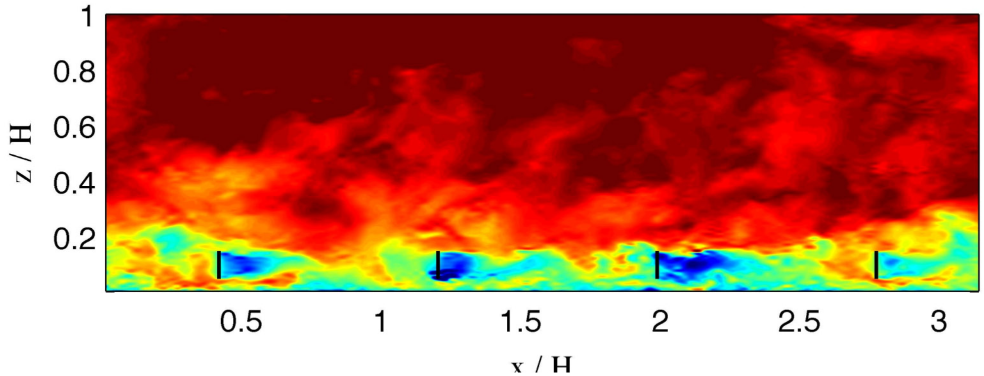

front-view

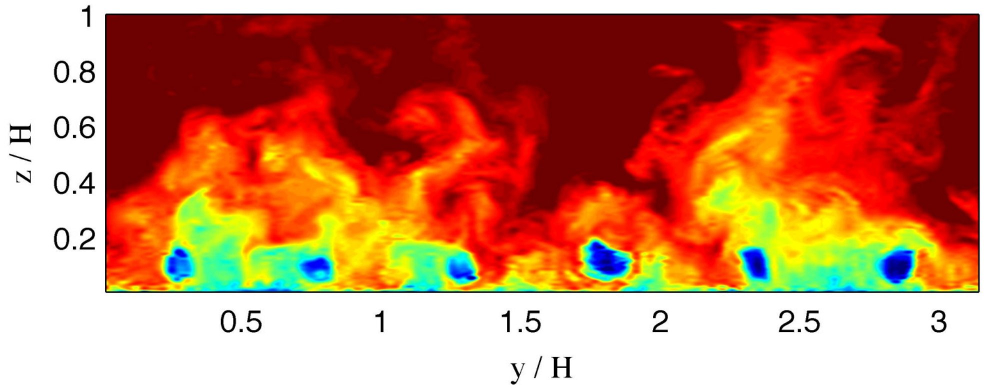

top-view

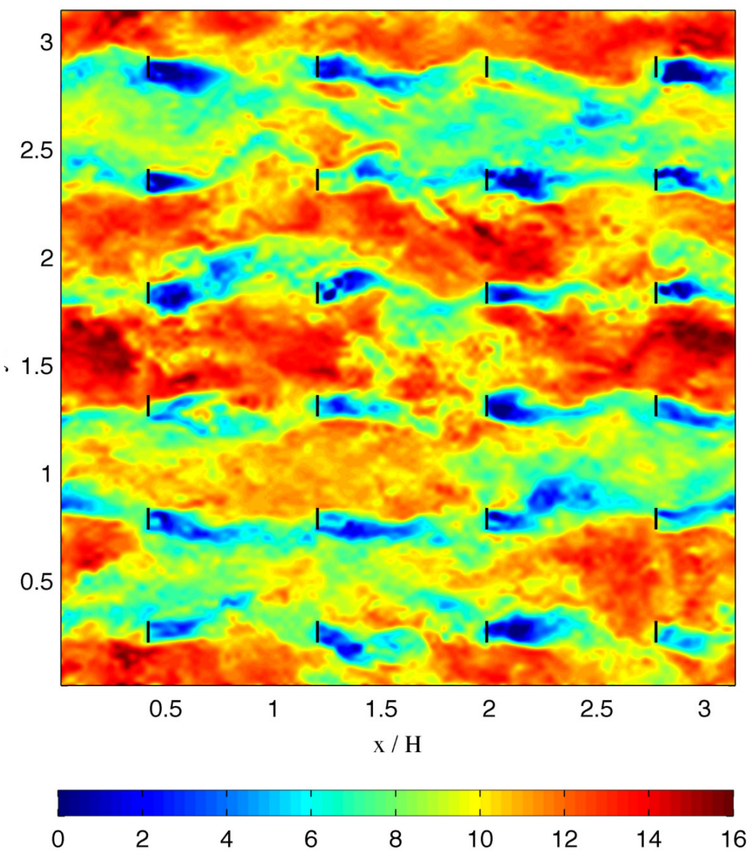

Simulations results:

Dynamic (scale-dependent) Smagorinsky coefficient:
increases in wake region, while decreases near wall

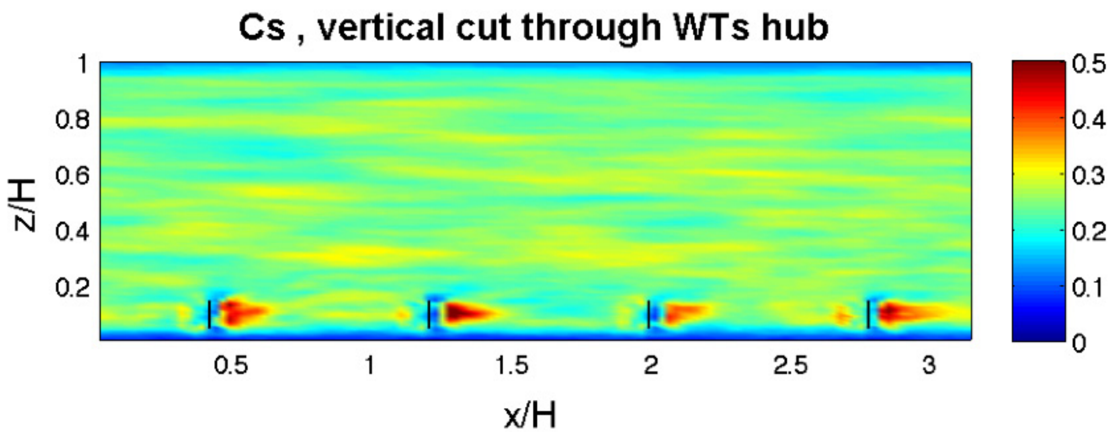

$$\left\langle c_s^2 \right\rangle^{1/2}$$

Comparison of wake profiles, regular Smagorinsy (with wall damping) and dynamic model:

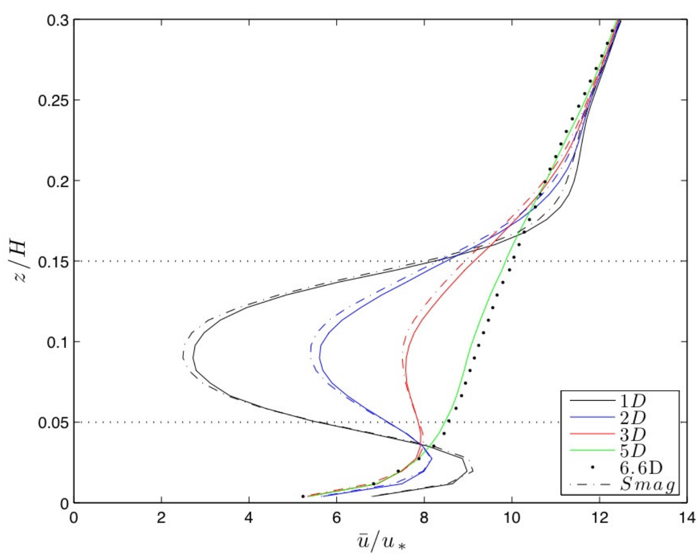

An aside about the “dynamic model” (for discussion)

Coupling “theory” with simulation:

$$\widetilde{u_i u_j} = \tilde{u}_i \tilde{u}_j + \left(\widetilde{u_i u_j} - \tilde{u}_i \tilde{u}_j \right)$$

Germano identity: constrain parameters based on fundamental physics (eg conservation of momentum fluxes)

$$\left\langle \widetilde{u_i u_j} \right\rangle = \left\langle \tilde{u}_i \tilde{u}_j \right\rangle + \left\langle \tau_{ij}^{\Delta} \right\rangle$$

same ↕ ↕ ↕

$$\left\langle \widehat{u_i u_j} \right\rangle = \left\langle \hat{u}_i \hat{u}_j \right\rangle + \left\langle \tau_{ij}^{b\Delta} \right\rangle$$

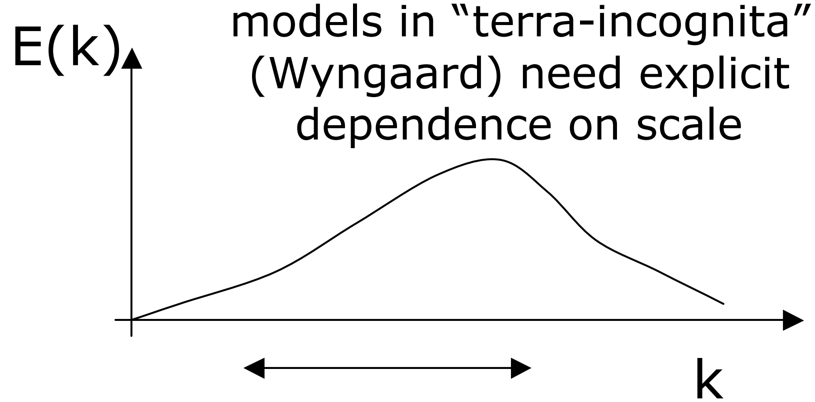

models in “terra-incognita” (Wyngaard) need explicit dependence on scale

Why not build such constraints directly into parameter choice for SGS model?

“Dynamic” is not restricted to Smagorinsky model !!!

Simulations results: horizontally averaged velocity profile *U(z)*

Mean velocity profile: $U(z) = \langle \overline{u} \rangle_{xy}$

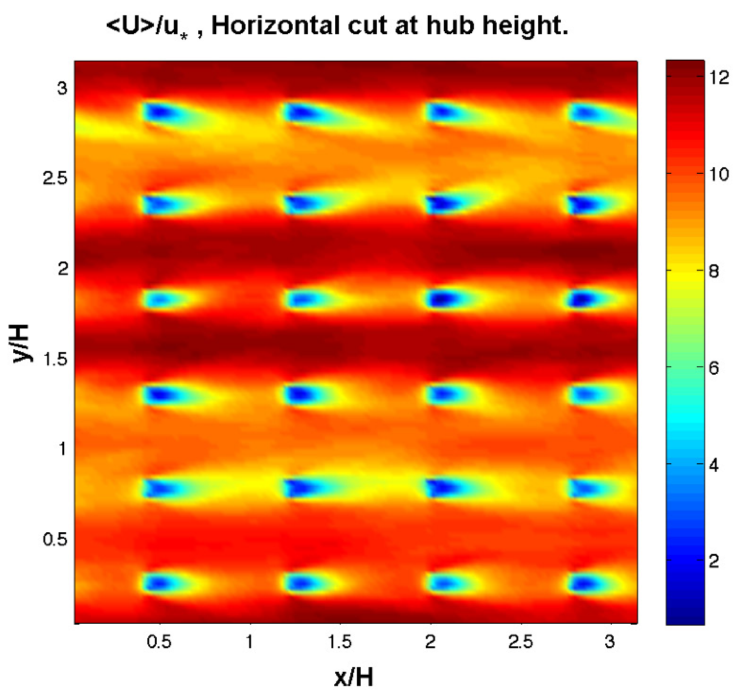

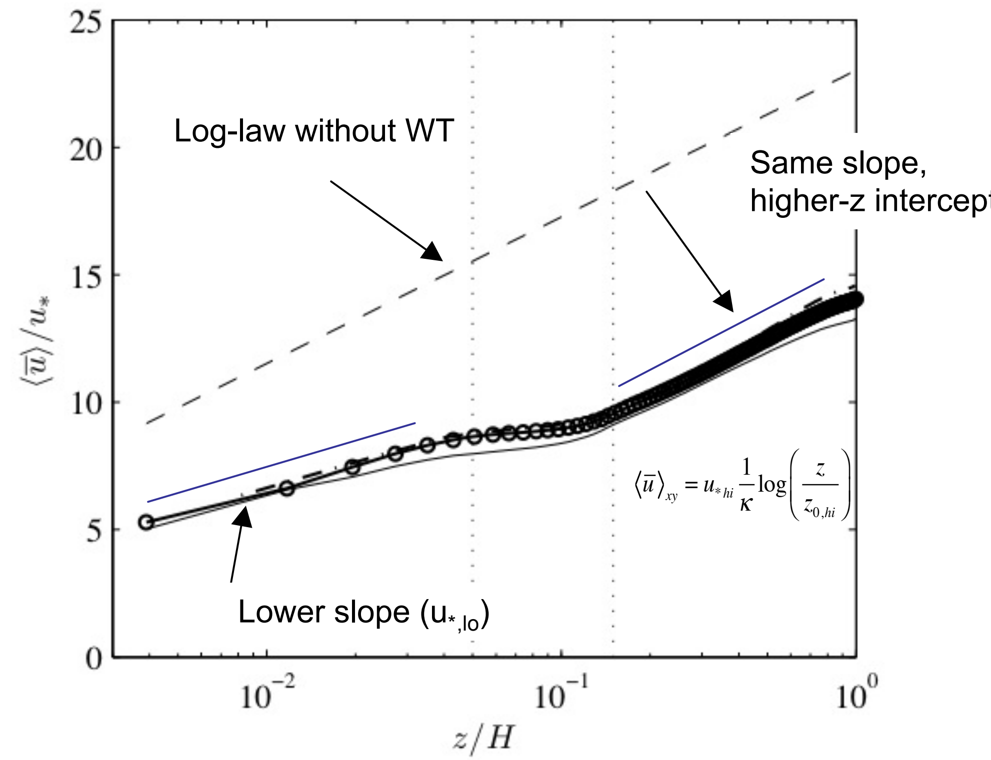

Important observation:

Two log-laws (as first hypothesized by Sten Frandsen, J. Wind Eng & Ind Appl 39, 1992)

Wind-tunnel measurements: mechanics of vertical KE entrainment??

Cal, Lebrón, Castillo, Kang & M.: "Experimental study of the horizontally averaged flow structure in a model wind-turbine array boundary layer", J. Renewable & Sustainable Energy **2** (2010) 013106

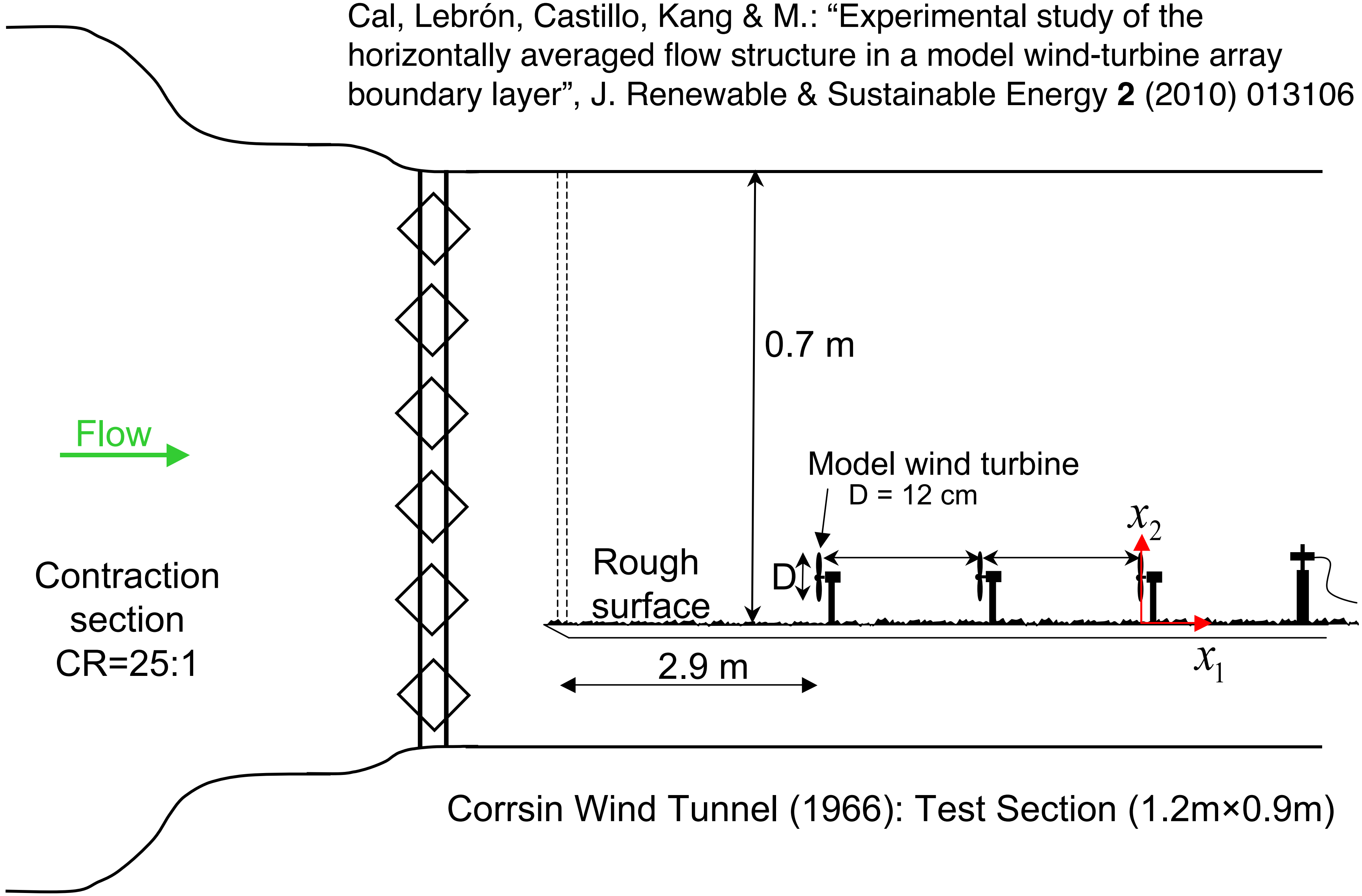

Corrsin Wind Tunnel (1966): Test Section (1.2m×0.9m)

Wind-tunnel measurements

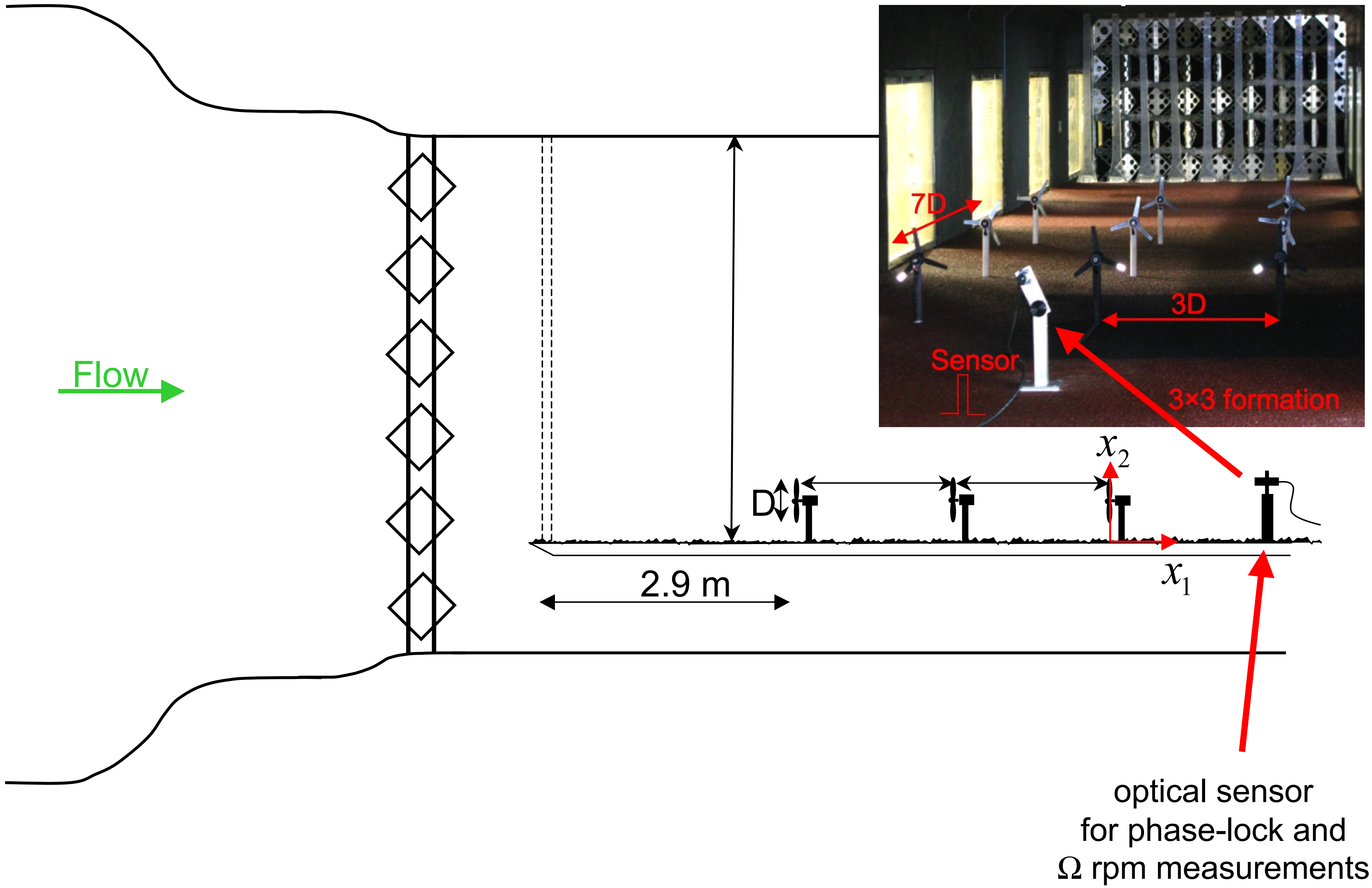

Stereo-PIV system

TSI System with:

- Double pulse Nd:YAG laser(120 mJ/pulse)
  - Laser sheet thickness of 1.2 mm
  - Time between pulses of 50 ms
  - Optical sensor external trigger for phase lock measurements
- Two high resolution cross/auto correlation digital CCD cameras with
  - a frame rate of 16 frames/sec.
  - Interrogation area of 20 cm by 20 cm

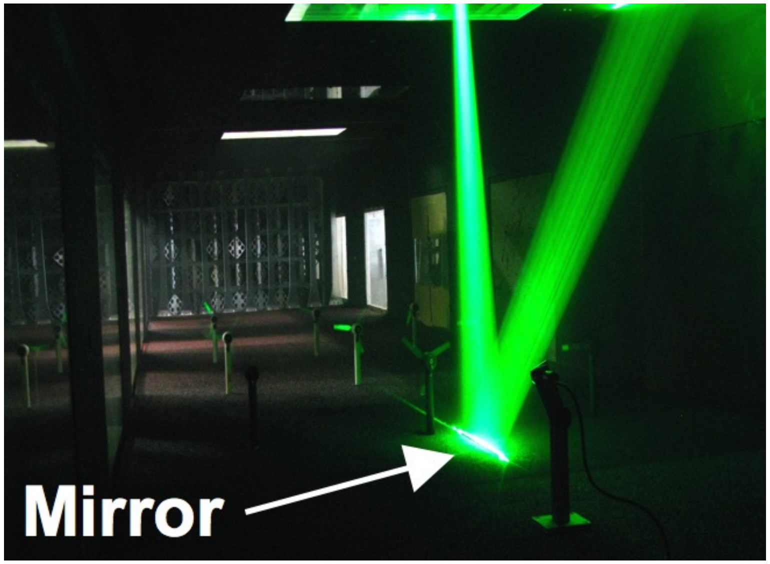

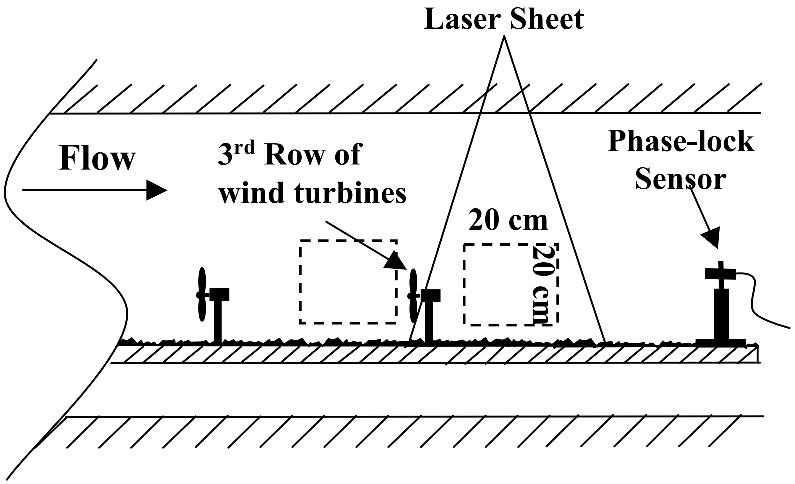

Velocity maps:

Mean streamwise velocity

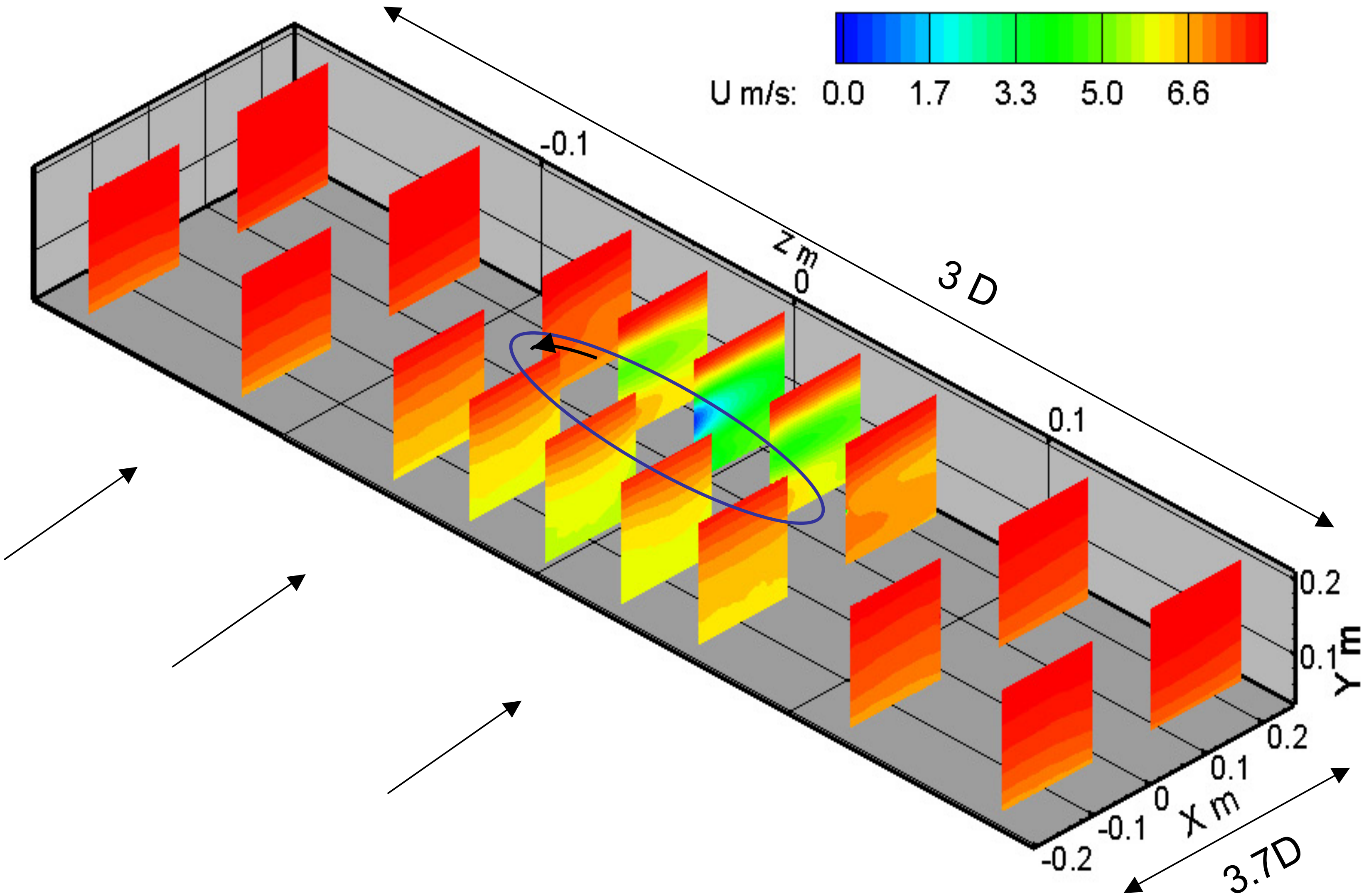

Horizontally (canopy) averaged profiles:

experiment

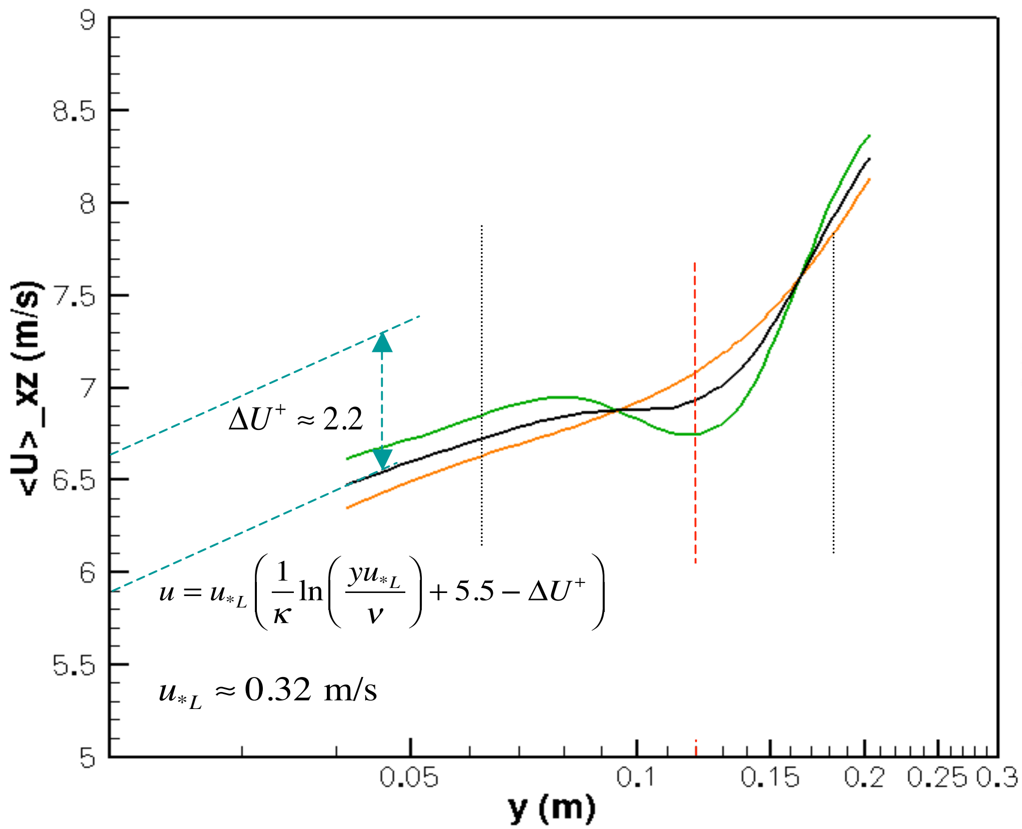

LES

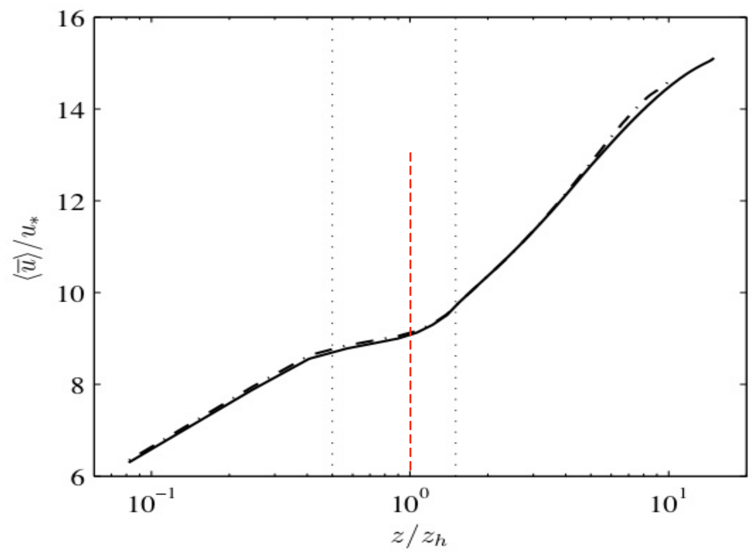

Suite of LES cases:

TABLE I. Summarizing parameters of the various LES cases. Between brackets is indicated which code is used: "L" refers to the KULeuven code and "J" refers to the JHU-LES code.

	s_x/s_y	s_x	$4s_xs_y/\pi$	N_t	$L_x \times L_y \times H$	$N_x \times N_y \times N_z$	$z_{0,\mathrm{lo}}$	C'_T	c'_{ft}
A1 (L)	1.5	7.85	52.36	4×6	$\pi\times\pi\times1$	128^3	10^{-4}	1.33	0.025
A2 (J)	1.5	7.85	52.36	4×6	$\pi\times\pi\times1$	128^3	10^{-4}	1.33	0.025
A3 (L)	1.5	7.85	52.36	8×6	$2\pi\times\pi\times1$	$128\times192\times61$	10^{-4}	1.33	0.025
A4 (L)	1.5	7.85	52.36	8×6	$2\pi\times\pi\times1.5$	$128\times192\times92$	10^{-4}	1.33	0.025
B (J)	1.5	7.85	52.36	4×6	$\pi\times\pi\times1$	128^3	10^{-4}	2.00	0.038
C (J)	1.5	7.85	52.36	4×6	$\pi\times\pi\times1$	128^3	10^{-4}	0.60	0.012
D (J)	1.5	7.85	52.36	4×6	$\pi\times\pi\times1$	128^3	10^{-3}	1.33	0.025
E (J)	1.5	7.85	52.36	4×6	$\pi\times\pi\times1$	128^3	10^{-5}	1.33	0.025
F (J)	1.5	7.85	52.36	4×6	$\pi\times\pi\times1$	128^3	10^{-6}	1.33	0.025
G (L)	1.5	15.7	209.4	4×3	$2\pi\times\pi\times1$	$128\times192\times61$	10^{-4}	1.33	0.0064
H (L)	1.5	6.28	33.51	10×8	$2\pi\times1.07\pi\times1$	$128\times192\times57$	10^{-4}	1.33	0.040
I (L)	1.5	5.24	23.27	12×9	$2\pi\times\pi\times1$	$128\times192\times61$	10^{-4}	1.33	0.057
J (L)	2	9.07	52.36	7×7	$2.02\pi\times1.01\pi\times1$	$128\times192\times61$	10^{-4}	1.33	0.025
K (L)	1	6.41	52.36	10×5	$2.04\pi\times1.02\pi\times1$	$128\times192\times60$	10^{-4}	1.33	0.025

Observations from the suite of LES:

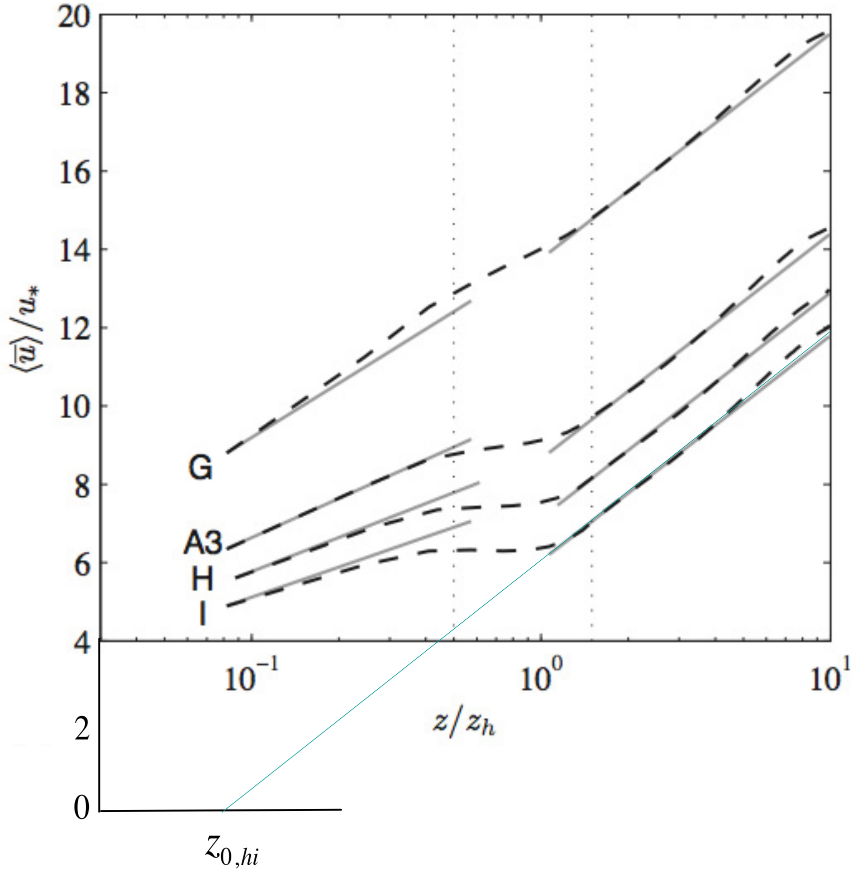

measure $z_{0,hi}$ from intercept

$$\langle \overline{u} \rangle_{xy} = u_{*hi} \frac{1}{\kappa} \log\left(\frac{z}{z_{0,hi}}\right)$$

(essentially the "Clauser plot" method)

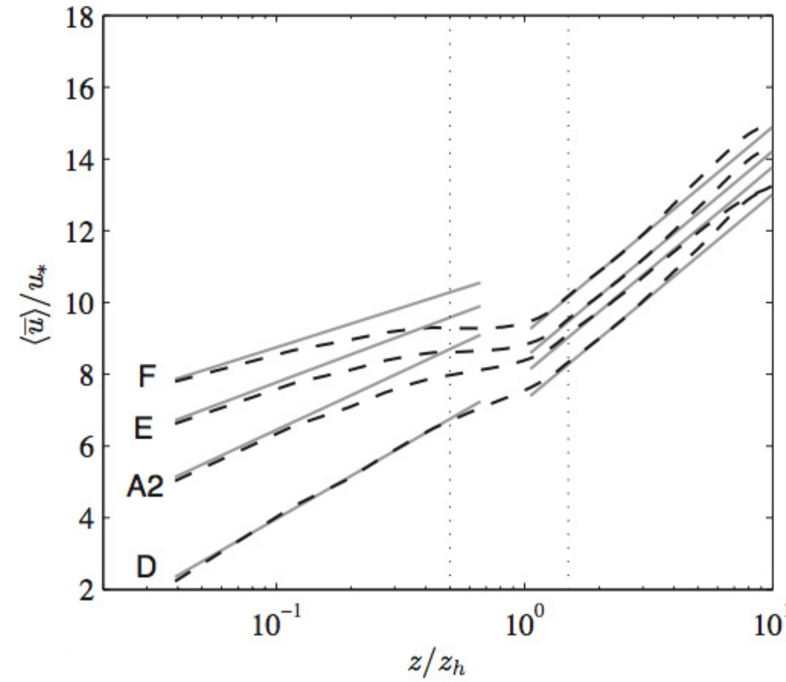

Crucial observation: 3 layers

The “fully developed” WTABL:

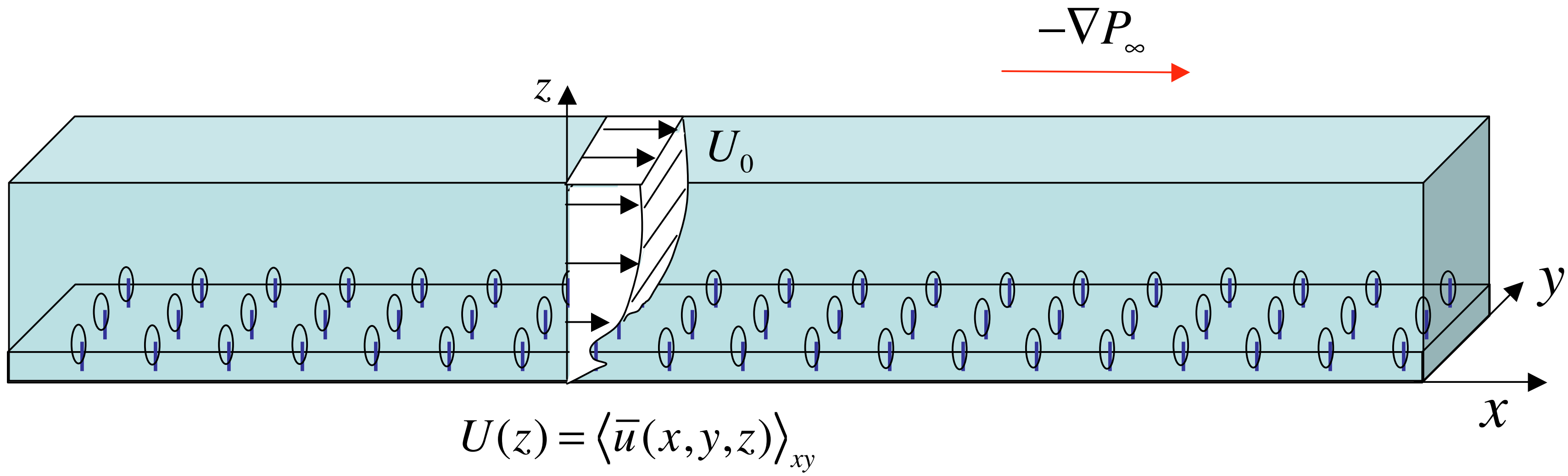

- 1-D Momentum theory:

$$0 = -\frac{1}{\rho}\frac{dp_\infty}{dx} + \frac{d}{dz}\left(-\langle \overline{u'w'} \rangle_{xy} - \langle \overline{u}''\overline{w}'' \rangle_{xy} \right) + \langle f_x \rangle_{xy}$$

thrust force due to WT

$$\overline{u}'' = \overline{u} - \langle \overline{u} \rangle_{xy}$$

Horizontal average
of turbulent Reynolds shear stress

We must include “correlations”
between mean velocity deviations
from their spatial mean
(Raupach et al. Appl Mech Rev **44**, 1991,
Finnigan, Annu Rev Fluid Mech **32**, 2000)

The fully developed WTABL: momentum theory

Horizontally averaged variables -- 2 layer model

S. Frandsen,
J. Wind Eng & Ind Appl **39**, 1992):

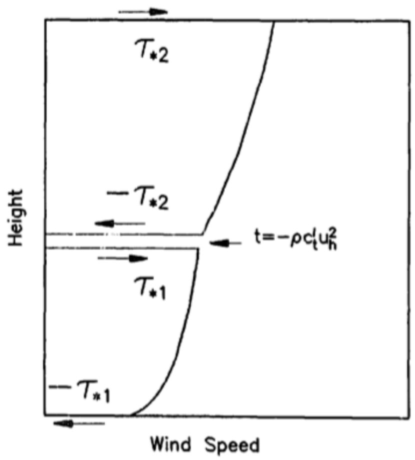

$$0 = -\frac{1}{\rho}\frac{dp_\infty}{dx} + \frac{d}{dz}\left(-\left\langle \overline{u'w'} \right\rangle_{xy} - \left\langle \bar{u}''\bar{w}'' \right\rangle_{xy}\right) + \left\langle f_x \right\rangle_{xy}$$

$$-\left\langle \overline{u'w'} \right\rangle_{xy}(z_{top}) \approx -\left\langle \overline{u'w'} \right\rangle_{xy}(z_{bottom}) + \frac{1}{2} C_T \frac{A_{disk}}{A_{xy}} U_R^2$$

$$u_{*\,hi}^2 \approx u_{*\,lo}^2 + \frac{1}{2} C_T \frac{\pi}{4 s_x s_y} U_R^2$$

Integrate 2 layers

$$\kappa u_* z \frac{\partial \langle \bar{u} \rangle}{\partial z} = u_*^2$$

$$s_x = \frac{L_x}{D}$$

$$s_y = \frac{L_y}{D}$$

$$z_{0,hi} = z_h \exp\left(-\kappa \left[\frac{\pi C_T}{8 s_x s_y} + \left(\frac{\kappa}{\ln(z_h / z_{0,ground})} \right) \right]^{-1/2} \right)$$

“Wake upgrade” to Frandsen’s model: 3rd layer

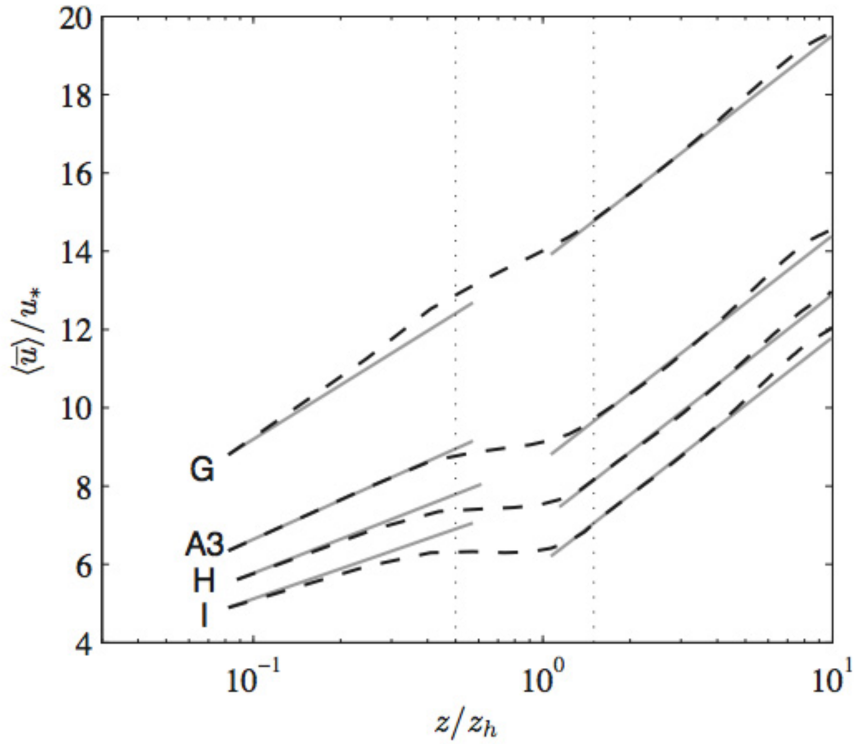

Integrate
3 layers

$$\left(\kappa u_* z_h + \nu_w\right)\frac{\partial\langle\overline{u}\rangle}{\partial z} = u_*^2$$

In wake, reduced slope:

$$\nu_w = \sqrt{\tfrac{1}{2}c_{ft}}\,\langle\overline{u}\rangle D$$

$$\nu_w^* = \frac{\sqrt{\tfrac{1}{2}c_{ft}}\,\langle\overline{u}(z_h)\rangle D}{\kappa u_* z_h} \approx 28\sqrt{\tfrac{1}{2}c_{ft}}$$

$$z_{0,hi} = z_h\left(1+\frac{D}{2z_h}\right)^{\beta}\exp\left(-\left[\frac{\pi C_T}{8\kappa^2 s_x s_y}+\left(\ln\left[\frac{z_h}{z_{0,ground}}\left(1-\frac{D}{2z_h}\right)^{\beta}\right]\right)^{-2}\right]^{-1/2}\right)$$

$$\text{where}\quad \beta = \frac{28\sqrt{\tfrac{1}{2}c_{ft}}}{1+28\sqrt{\tfrac{1}{2}c_{ft}}},$$

Comparison of LES results with models:

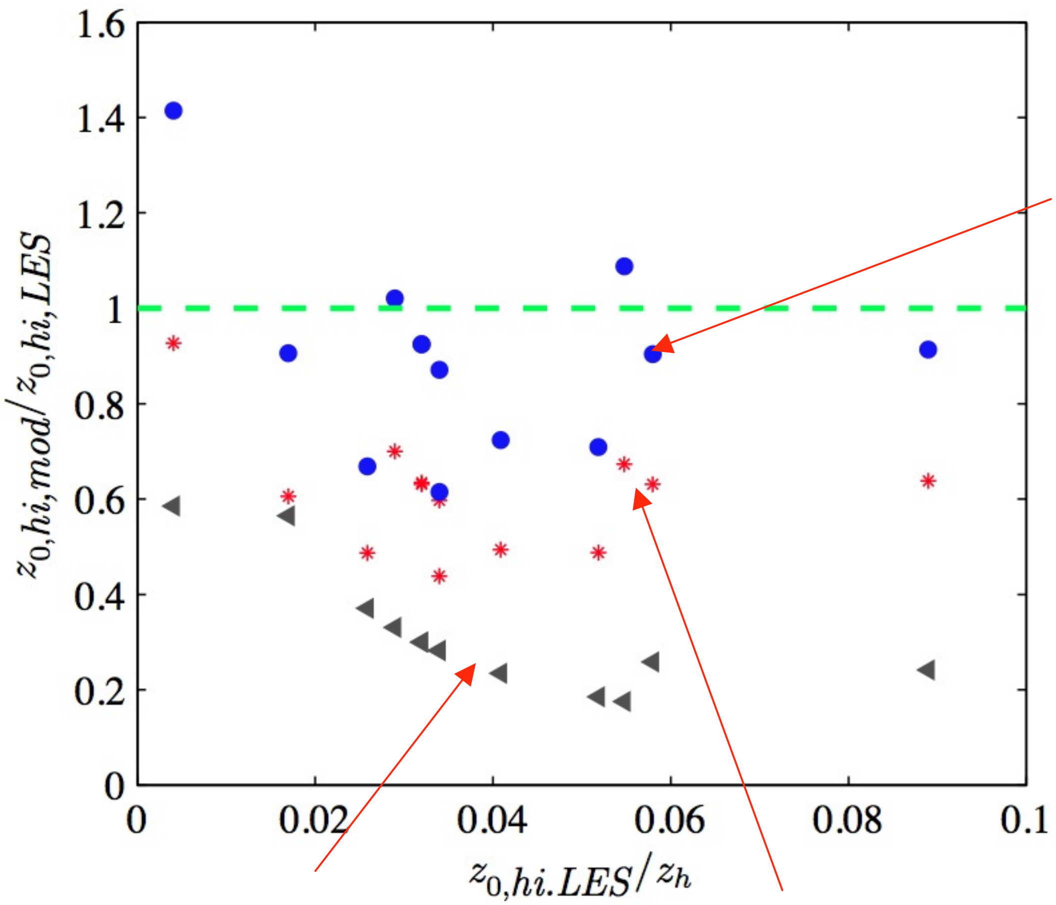

Circles: improved Frandsen model
Calaf, Meneveau & Meyers,
(Phys. Fluids 2010, **22**)

$$z_{0,hi} = z_h \left(1+\frac{D}{2z_h}\right)^{\beta} \exp\left(-\left[\frac{\pi C_T}{8\kappa^2 s_x s_y}+\left(\ln\left[\frac{z_h}{z_{0,ground}}\left(1-\frac{D}{2z_h}\right)^{\beta}\right]\right)^{-2}\right]^{-1/2}\right)$$

where $\beta = \frac{\nu_w^*}{1+\nu_w^*}$, and $\nu_w^* = \frac{\nu_T}{\kappa u_* z_h}$, eddy viscosity due to wake

Triangles: Lettau formula

Asterisks: Frandsen et al. (2006) formula

$$z_{0,hi} = z_h \exp\left(-\kappa\left[\frac{\pi C_T}{8 s_x s_y}+\left(\frac{\kappa}{\ln(z_h / z_{0,ground})}\right)\right]^{-1/2}\right)$$

Example application of fully developed WTABL concepts and z_0: GCMs, mesoscale models, etc…

Keith et al. "The influence of large-scale wind power on climate" PNAS (2004)

Barrie & Kirk-Davidoff: "Weather response to management of large Wind turbine array", Atmos. Chem. Phys. Discuss. **9**, 2917–2931, 2009

Use z_0 ~ 0.8 m - using "Lettau's formula" (ad-hoc geometric arguments…)

Grid-spacings 100's of km, first vertical point ~ 80m

"horizontally averaged structure"

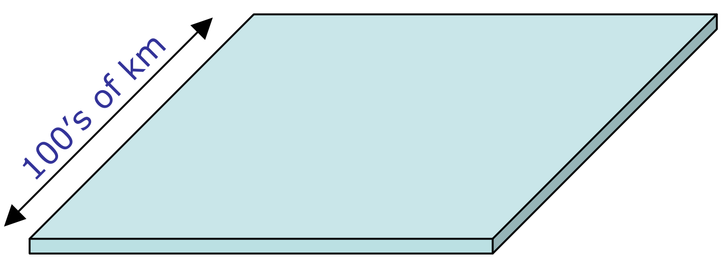

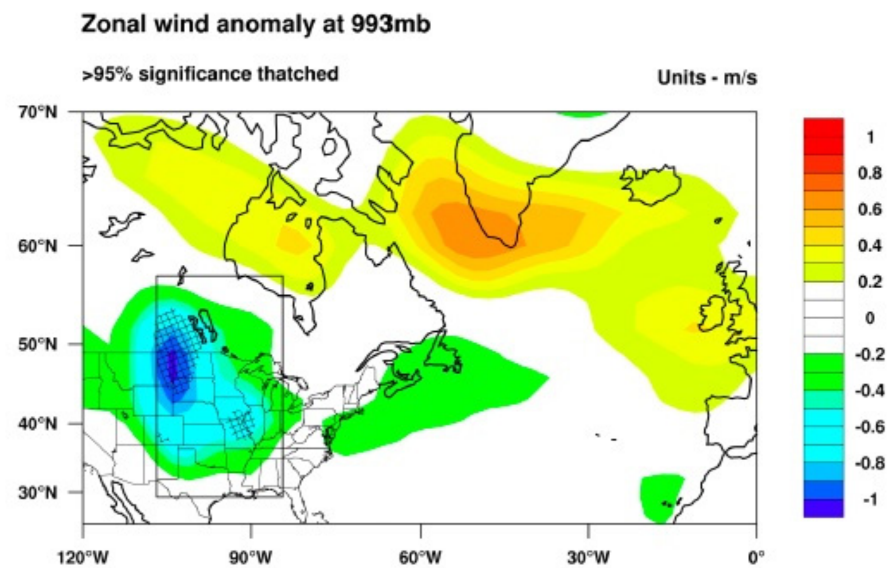

Fig. 1. 993 mbar zonal wind anomaly. The mean difference in the eastward wind in the lowest model level between the control and perturbed model runs highlights regions of atmospheric modification. Regions where significance exceeds 95%, as determined by a Student's t-test, are thatched. The wind farm is located within the rectangular box over the central United States and central Canada. Areas of the wind farm located over water are masked out during the model runs.

The "fully developed" WTABL: Forcing by geostrophic wind

Above ABL (in mid-latitudes): geostrophic balance $2\boldsymbol{\Omega}\times\mathbf{G}-\frac{1}{\rho}\nabla P\approx 0$

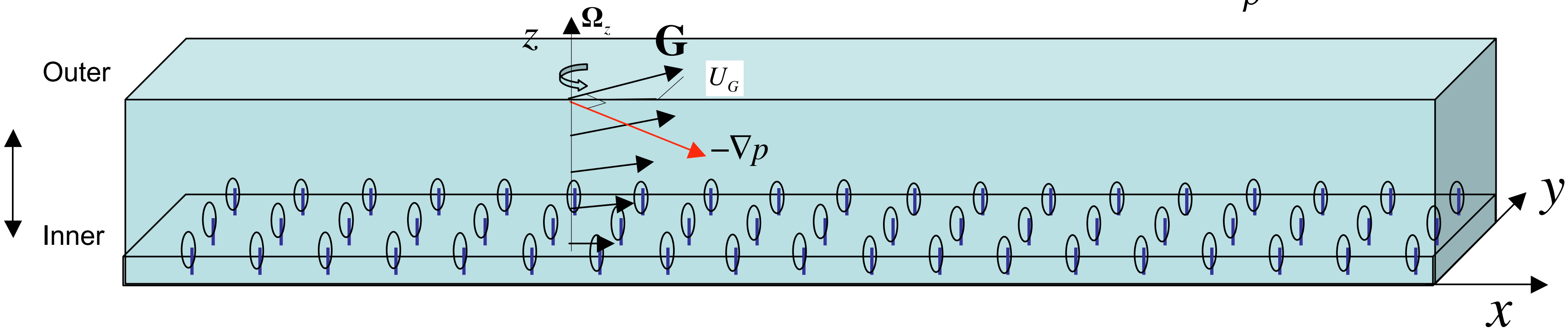

Coupled through a stress $(u_*)^2$:

Outer length-scale: $L=\frac{u_*}{f}$ $\quad f=2\Omega\sin\phi\approx 10^{-4}s^{-1}$ (mid-latitudes)

Inner length-scale: z_0

Inner-outer matching: $\frac{u(z)}{u_*}=\frac{1}{\kappa}\ln\left(\frac{z}{z_0}\right)$ $\quad \frac{G}{u_*}=\sqrt{A^2+\left[\frac{1}{\kappa}\ln\left(\frac{u_*}{fz_0}\right)-C\right]^2}$

Given G and z_0 ----> find $u_{*,hi}$ and H

Using the roughness model for array optimization - find s-opt:

Driving forces is geostrophic wind G (assuming large but not regional-scale WT, i.e. assume wind farm does not affect *G*)

$$P^+ = \frac{P}{\frac{\rho}{2}(s_x s_y D^2)G^3} = \frac{\pi C_T'}{4 s_x s_y}\left(\frac{U_d}{G}\right)^3 = \frac{\pi C_T'}{4 s_x s_y}\left(\frac{u_{*,hi}}{G}\right)^3\left(\frac{U_d}{u_{*,hi}}\right)^3$$

Classical ABL relationship
(Tennekes & Lumley, 1972) - *C=4.5, A=11.25*

$$\frac{G}{u_{*,hi}} = \sqrt{A^2 + \left[\frac{1}{\kappa}\ln\left(\frac{u_{*,hi}}{G}\frac{z_h}{z_{0,hi}}Ro_h\right) - C\right]^2}$$

$$Ro_h = \frac{G}{f z_h} \approx 2{,}000$$

typical hub-height Rossby number

$$\frac{z_{0,hi}}{z_h} = \left(1 + \frac{D}{2z_h}\right)^{\beta} \exp\left(-\left[\frac{\pi C_T}{8\kappa^2 s_x s_y} + \left(\ln\left[\frac{z_h}{z_{0,ground}}\left(1 - \frac{D}{2z_h}\right)^{\beta}\right]\right)^{-2}\right]^{-1/2}\right)$$

Using the roughness model for array optimization - find s-opt:

$$P^{+} = \frac{P}{\frac{\rho}{2}(s_x s_y D^2)G^3} = \frac{\pi C_T'}{4 s_x s_y}\left(\frac{U_d}{G}\right)^3 = \frac{\pi C_T'}{4 s_x s_y}\left(\frac{u_{*,hi}}{G}\right)^3 \left(\frac{U_d}{u_{*,hi}}\right)^3$$

$$u_{*\,hi}^2 \approx u_{*\,lo}^2 + \frac{1}{2} C_T' \frac{\pi}{4 s_x s_y} U_d^2$$

$$\frac{U_d}{u_{*hi}} = \sqrt{\frac{1 - \frac{u_{*\,hi}^2}{u_{*\,lo}^2}}{\frac{1}{2} C_T \frac{\pi}{4 s_x s_y}}} \qquad \frac{u_{*\,hi}}{u_{*\,lo}} = \frac{\ln\left[\frac{z_h}{z_{0,hi}}\left(1 + \frac{D}{2 z_h}\right)^{\beta}\right]}{\ln\left[\frac{z_h}{z_{0,lo}}\left(1 - \frac{D}{2 z_h}\right)^{\beta}\right]}$$

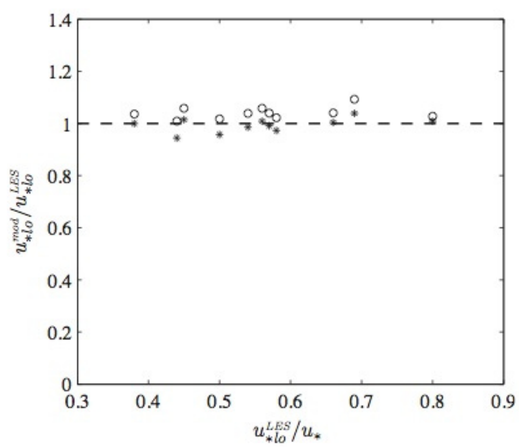

For given *s*, $z_{0,lo}$, *D*, z_h, C_T evaluate P^+

Divide by P^+ of single WT

Using the roughness model for array optimization - find s-opt:

For given s, $z_{0,lo}$, D, z_h, C_T evaluate P
divide by P_∞ of single WT ($z_{0,hi} = z_{0,lo}$ case)

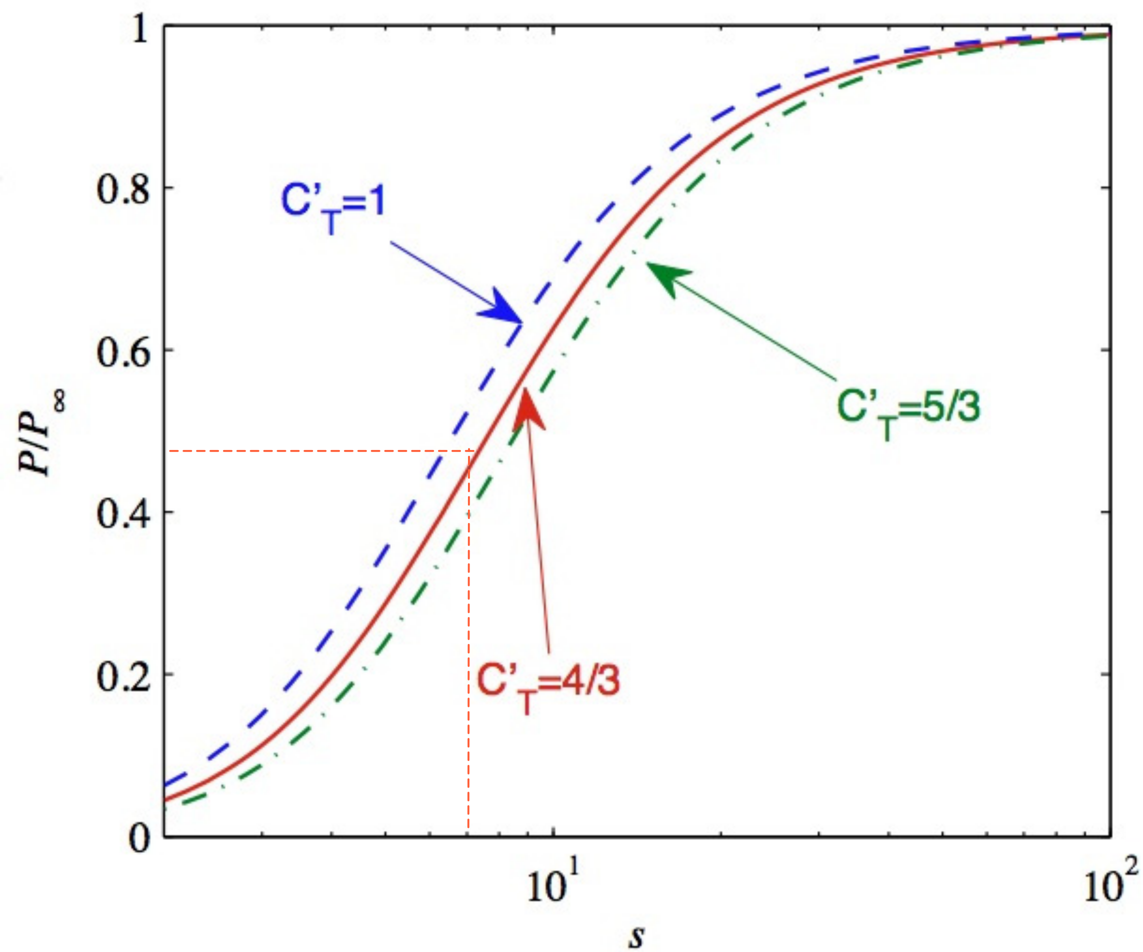

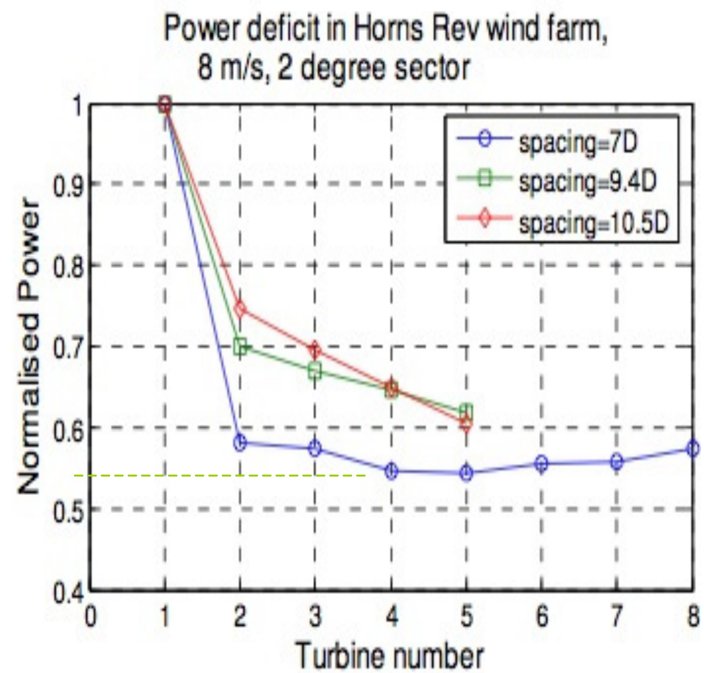

~ 48-55% power degradation at 7D

Using the roughness model for array optimization - find s-opt:

Optimization:

consider total $Cost = Cost_{land}$ [\$/m^2] x $S + Cost_{turb}$ [\$]

Define dimensionless ratio:

$$\alpha = \frac{Cost_{turb} / \left(\frac{\pi}{4} D^2\right)}{Cost_{land}}$$

Power per unit cost:

$$P^* = \frac{P}{Cost_{turb} / (s_x s_y D^2) + Cost_{land}} \propto \frac{C_T'}{4 s_x s_y / \pi + \alpha} \left(\frac{u_{*,hi}}{G}\right)^3 \left(\frac{U_d}{u_{*,hi}}\right)^3$$

(region II)

Using the roughness model for array optimization - find s-opt:

~ P* (arbitrary vertical scale):

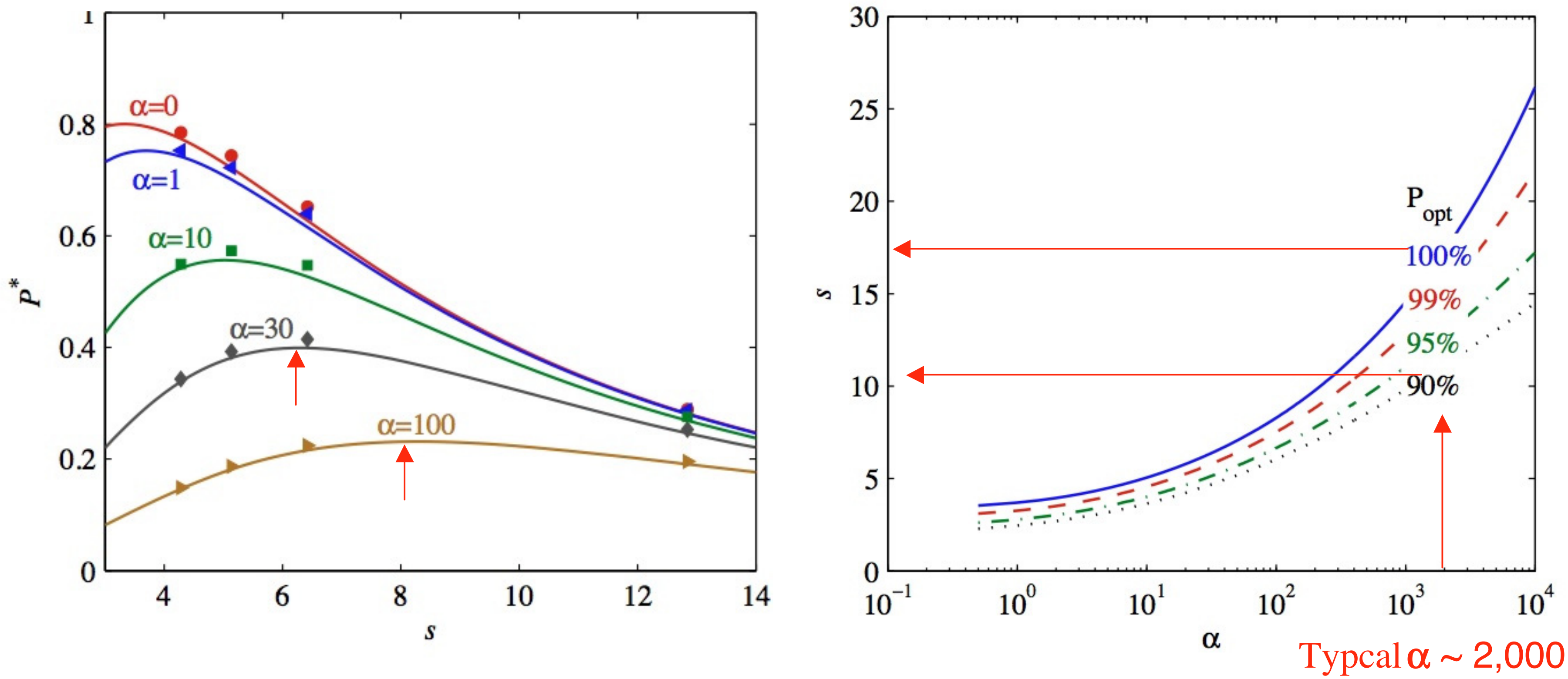

At common s ~ 7D, 10-20% suboptimal
possible reason for "array underperformance" ?

Meyers & Meneveau, 2010
(preprint, submitted to Wind Energy)

Application 2:

Agriculture: What is the isolation distance to avoid cross-polination?

Collaboration with **Marcelo Chamecki** (Penn State U)

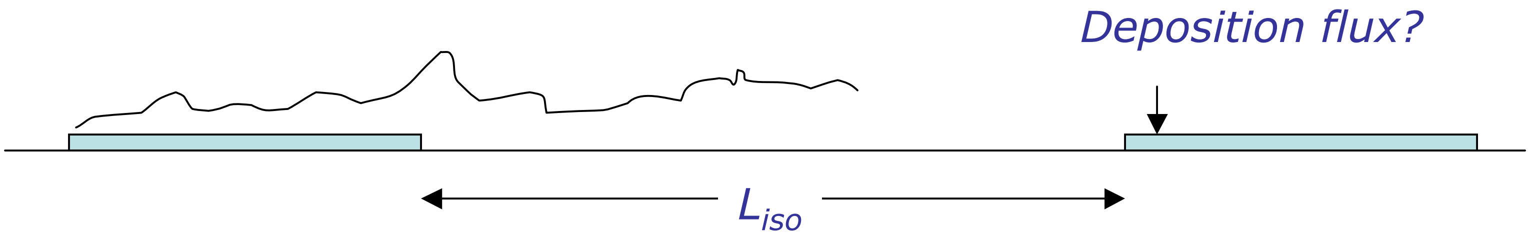

LES:

Eulerian approach C(x,y,z,t)

Vertical settling velocity w_s

Scale-dep dynamic eddy-viscosity eddy-diffusivity SGS

Log-law type boundary condition

For C, log-law, corrected by settling velocity

$$\frac{\partial \tilde{C}}{\partial t} + \left(\tilde{\mathbf{u}} - w_s \mathbf{e}_3\right)\cdot\nabla\tilde{C} = \nabla\cdot\left(\left(C_{s-dyn}\Delta\right)^2 |\tilde{\mathbf{S}}|\, \tilde{C}\right)$$

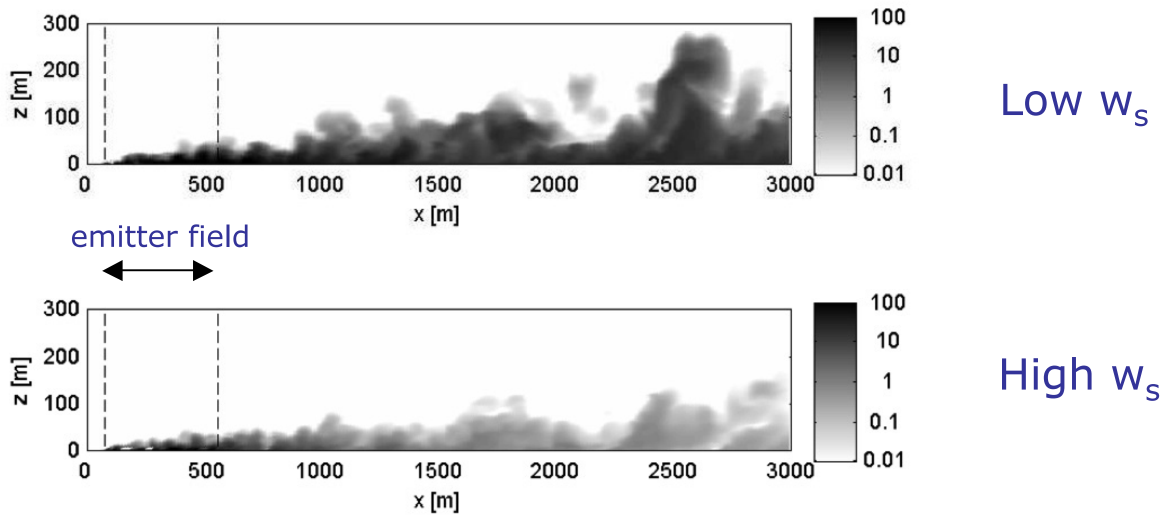

FIGURE 4. Snapshots of iso-contours of resolved pollen concentration (on x-z plane) for (a) $\gamma = 0.125$ and (b) $\gamma = 0.625$. Dashed lines indicate the horizontal extent of the source field.

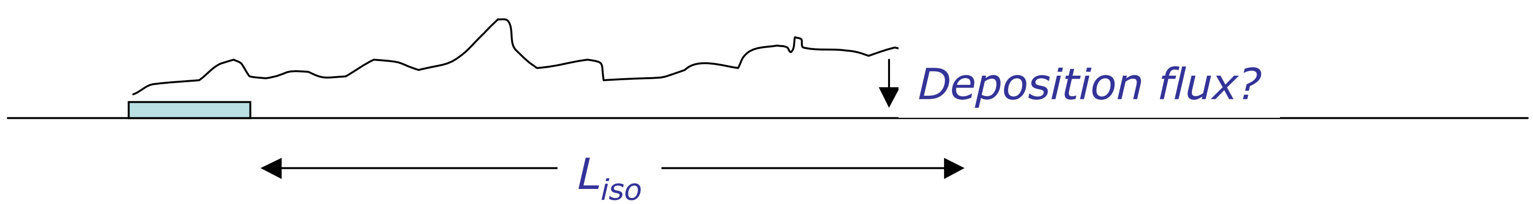

LES results:

Downstream evolution of concentration profiles

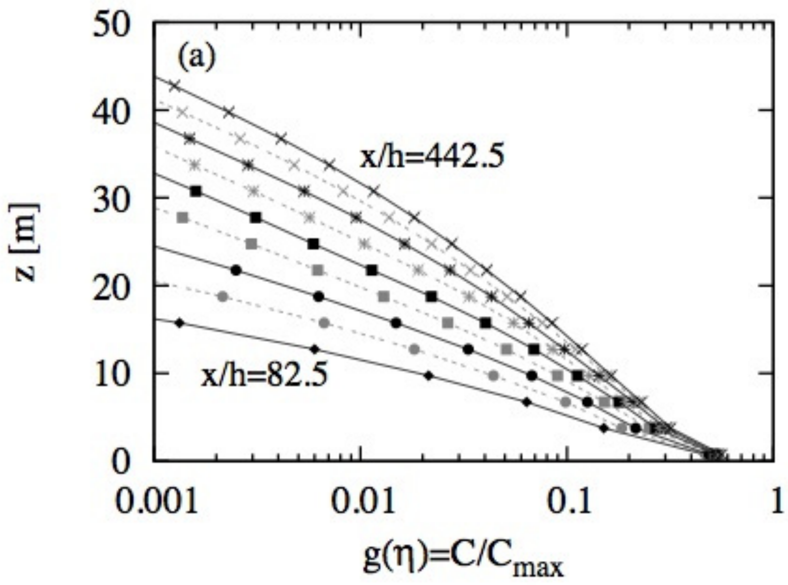

Downstream evolution of deposition flux

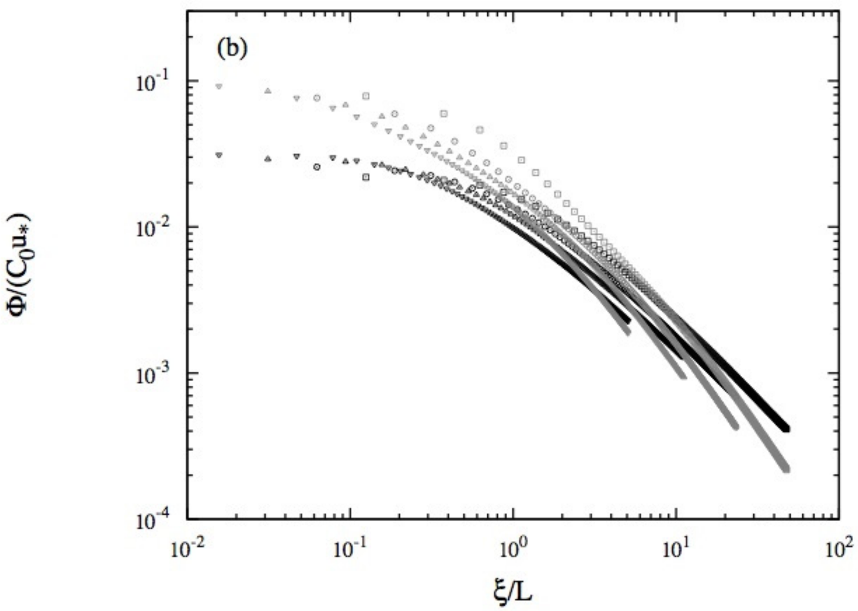

1-D "reduction" (back to early 1900s) - vertical profile

$$\overline{u}(z)\frac{\partial \overline{C}}{\partial x} - w_s\frac{\partial \overline{C}}{\partial z} = \frac{\partial}{\partial z}\left(K_c(z)\frac{\partial \overline{C}}{\partial z}\right),$$

$$\overline{C}(x=0,z)=0$$
$$\overline{C}(x,z\to\infty)=0$$
$$\overline{C}(x,z=z_{0,c})=\overline{C}_0,$$

$$\overline{u}(z) = u_* C_p\left(\frac{z}{z_o}\right)^m, \quad K_c(z) = \frac{\kappa u_* z}{\mathrm{Sc}},$$

$$z\frac{\partial^2 \overline{C}}{\partial z^2} + (1+\gamma)\frac{\partial \overline{C}}{\partial z} - \frac{\mathrm{Sc}\,C_p}{\kappa}\left(\frac{z}{z_o}\right)^m\frac{\partial \overline{C}}{\partial x} = 0,$$

$$\frac{d^2 g}{d\eta^2} + (1+\gamma)\frac{1}{\eta}\frac{dg}{d\eta} + \frac{\mathrm{Sc}\,C_p}{\kappa z_0^m}\left(\delta_c^m\frac{d\delta_c}{dx}\right)\eta^m\frac{dg}{d\eta} = 0.$$

$$\frac{\overline{C}(x,z)}{\overline{C}_{max}(x)} = g(\eta),$$

$$g'' + \left[\frac{(1+\gamma)}{\eta} + C_1(\gamma)\eta^m\right]g' = 0,$$

$$g(\eta) = -C_I\frac{1}{m+1}\left(\frac{C_1(\gamma)}{m+1}\right)^{\gamma/(m+1)}\int_{\frac{C_1(\gamma)}{m+1}\eta^{m+1}}^{\infty} t^{-[1+\gamma/(m+1)]}\exp[-t]\,dt$$

$$g(\eta) = \frac{\Gamma\left(-\frac{\gamma}{m+1}, \frac{C_1(\gamma)}{m+1}\eta^{m+1}\right)}{\Gamma\left(-\frac{\gamma}{m+1}, \frac{C_1(\gamma)}{m+1}\eta_0^{m+1}\right)},$$

Similarity solution for any γ (Rouse #)

Deposition downstream of field:

$$\frac{d^2 f}{d\eta^2} + (1+\gamma)\frac{1}{\eta}\frac{df}{d\eta} + \frac{\mathrm{Sc}C_p}{\kappa z_o^m}\left(\delta_c^m \frac{d\delta_c}{d\xi}\right)\eta^m \frac{df}{d\eta} - \frac{\mathrm{Sc}C_p}{\kappa z_o^m}\left(\frac{\delta_c^{m+1}}{\overline{C}_{max}}\frac{d\overline{C}_{max}}{d\xi}\right)\eta^{m-1} f = 0. \quad (2.30)$$

Since both δ_c and $\overline{C}_{max}$ depend on ξ, constraint (2.14) still has to be satisfied. There is one additional requirement for the existence of a similarity solution, namely that

$$C_3(\gamma) = -\frac{\mathrm{Sc}C_p}{\kappa z_o^m}\left(\frac{\delta_c^{m+1}}{\overline{C}_{max}}\frac{d\overline{C}_{max}}{d\xi}\right) \quad (2.31)$$

is independent of downstream distance. The final ODE contains three terms, two of which are similar to (2.15), and is given by

$$f'' + \left[\frac{(1+\gamma)}{\eta} + C_2(\gamma)\eta^m\right] f' + C_3(\gamma)\eta^{m-1} f = 0 \quad (2.32)$$

where $C_2(\gamma)$ is used instead of $C_1(\gamma)$ to indicate that the function may actually be different from the one obtained in the previous section.

Equation (2.24) should still be valid if a non-zero initial boundary layer height $\delta_c(\xi = 0) = \delta_L$ is imposed

$$\delta_c(\xi) = \left[\delta_L^{m+1} + C_2(\gamma)\frac{\kappa z_o^m}{\mathrm{Sc}C_p}(m+1)\xi\right]^{\frac{1}{m+1}}. \quad (2.33)$$

Replacing this expression for $\delta_c(\xi)$ into equation (2.31) and solving for $\overline{C}_{max}(\xi)$ yields

$$\overline{C}_{max}(\xi) = \overline{C}_{ini}(\gamma)\left[1 + C_2(\gamma)\frac{\kappa(m+1)}{\mathrm{Sc}C_p}\left(\frac{z_o}{\delta_L}\right)^m \frac{\xi}{\delta_L}\right]^{-\frac{C_3(\gamma)}{(m+1)C_2(\gamma)}} \quad (2.34)$$

where the initial condition $\overline{C}_{max}(\xi = 0) = \overline{C}_{ini}(\gamma)$ was used. Equation (2.34) can be written as

$$\overline{C}_{max}(\xi) = \overline{C}_{ini}(\gamma)\left[1 + \frac{1}{b(\gamma)}\frac{\xi}{\delta_L}\right]^{-\beta(\gamma)} \quad (2.35)$$

where the following definitions were used

$$b(\gamma) = \left[C_2(\gamma)\frac{\kappa(m+1)}{\mathrm{Sc}C_p}\left(\frac{z_o}{\delta_L}\right)^m\right]^{-1} \quad (2.36)$$

$$\beta(\gamma) = \frac{C_3(\gamma)}{(m+1)C_2(\gamma)}. \quad (2.37)$$

$$\gamma = \frac{Sc}{\kappa}\frac{w_s}{u_*}$$

$$\Phi(\xi) = \left[w_s\overline{C} + K_c\frac{\partial\overline{C}}{\partial z}\right]_{z=z_{0,c}}$$

$$\frac{\Phi(\xi)}{\overline{C}_{max}(\xi)u_*} = \frac{w_s}{u_*}\left[f + \frac{\eta}{\gamma}\frac{df}{d\eta}\right]_{\eta=\eta_0}$$

$$\Phi(\xi) = a(\gamma)\left[1 + \frac{1}{b(\gamma)}\frac{\xi}{\delta_L}\right]^{-\beta(\gamma)}$$

δ_L is proper length-scale for deposition flux, not L

Comparison with LES:

$$\gamma = \frac{Sc}{\kappa}\frac{w_s}{u_*} = 0.125$$

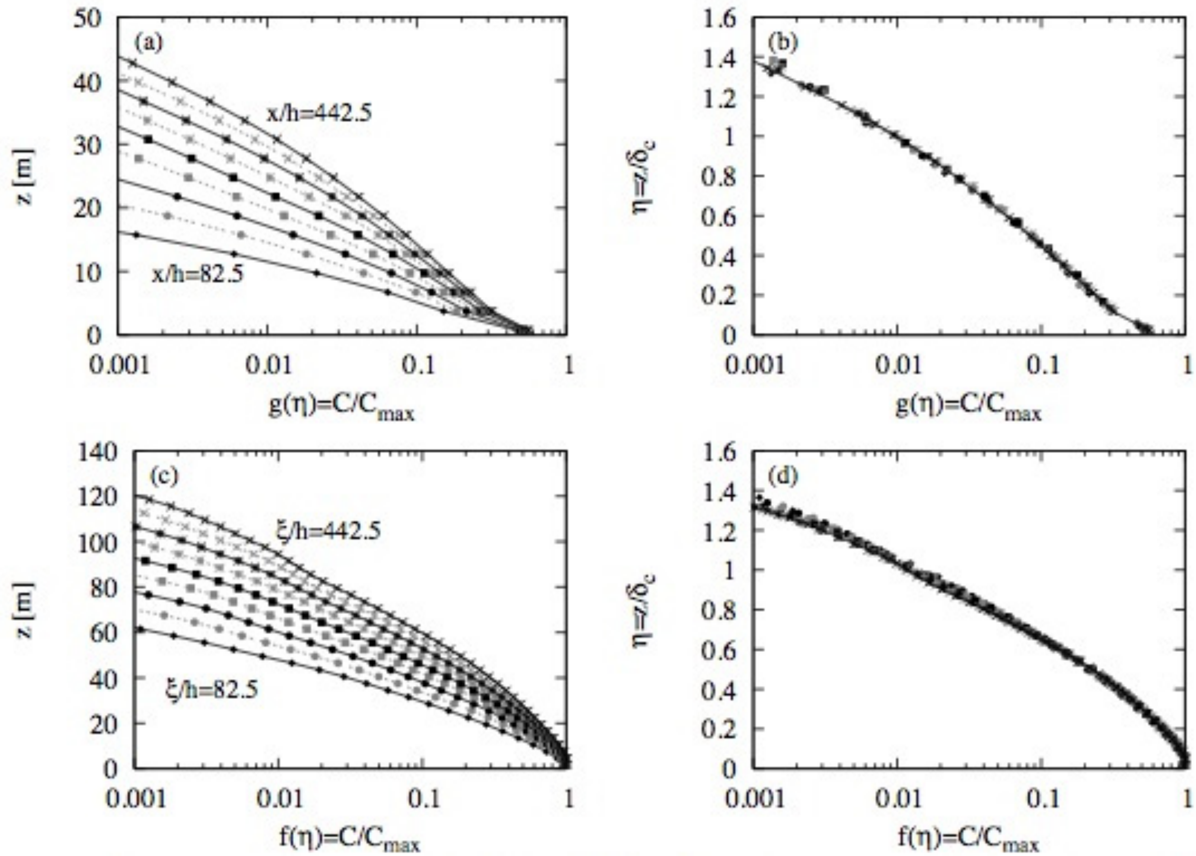

Over field

Downstream

FIGURE 5. Average pollen concentration profiles above the source field normalized by local maximum concentration at different distances from the leading edge x/h (from $x/h = 82.5$ to $x/h = 442.5$ in increments of 50) for $\gamma = 0.125$. (a) Plotted against height above the ground and (b) against dimensionless height η illustrating collapse consistent with self-preservation. Panels (c) and (d) are similar for concentration profiles downstream from the source at different distances from the trailing edge ξ/h.

Scaling of deposition flux: field edge δ instead of L

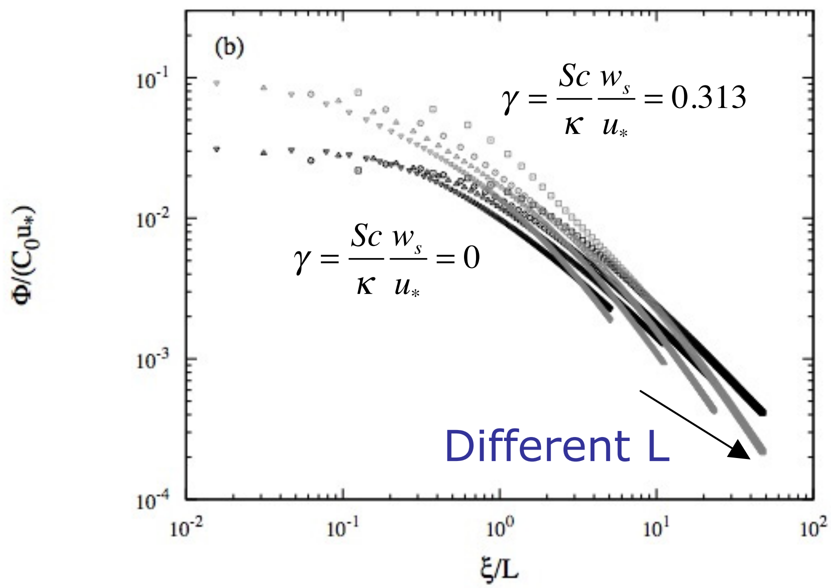

Traditional approach
(current rules)

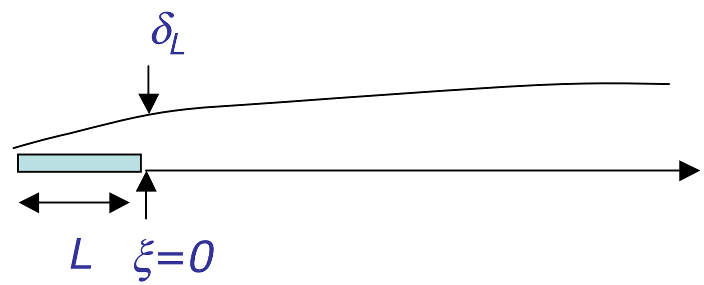

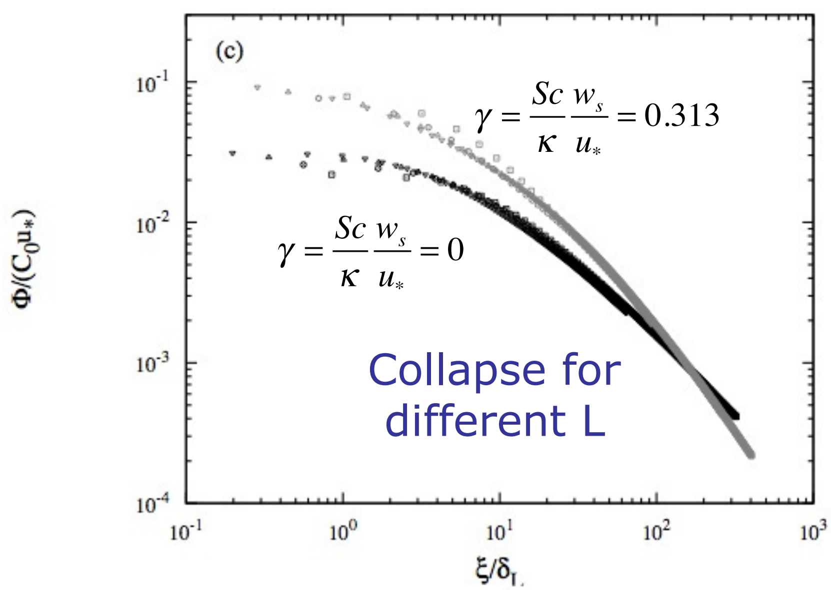

Scaling with δ_L

Isolation distance as function of flux threshold:

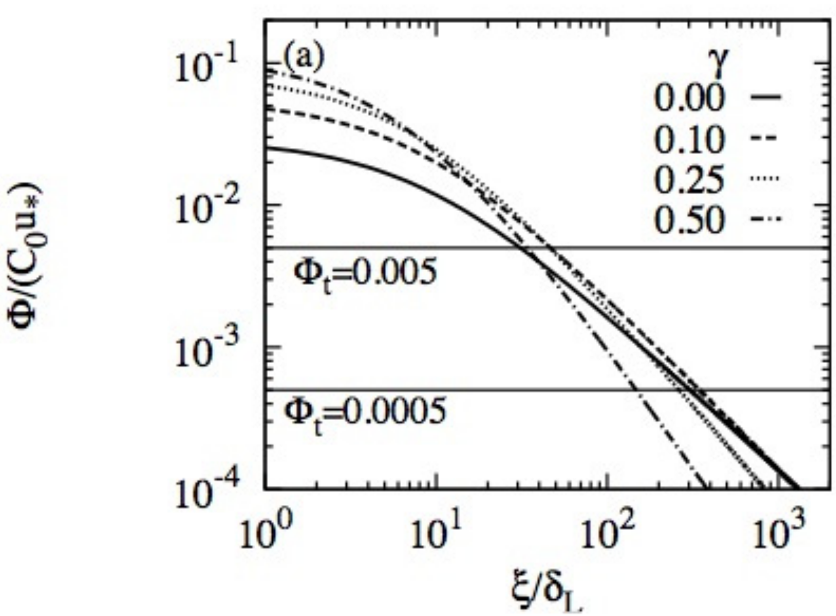

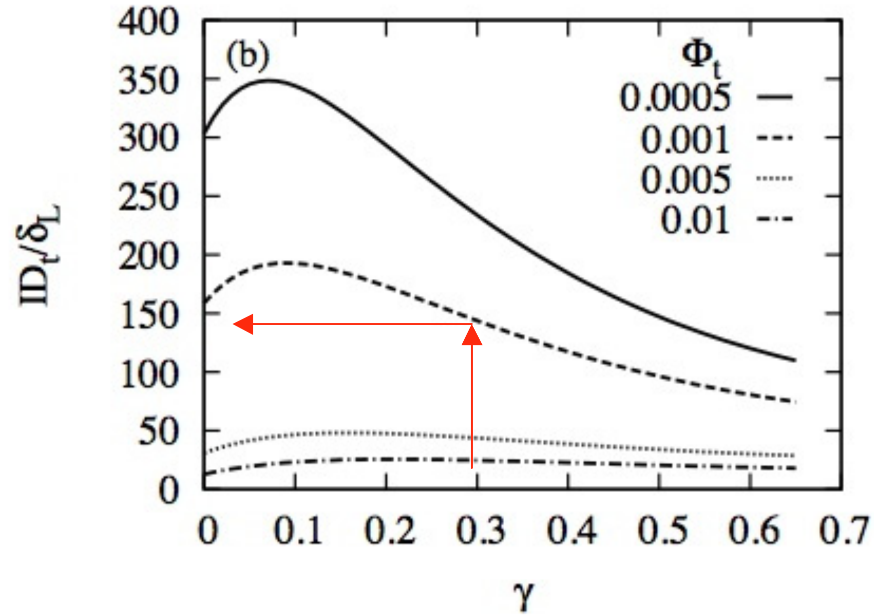

E.g., w_s=0.06 m/s (d=40 μm), u*=0.5 m/s, Sc=1, κ=0.4, $\gamma = \frac{Sc}{\kappa}\frac{w_s}{u_*} = 0.3$

L=500m -> δ_L=30m, E.g., $\Phi=10^{-3}$ -> ID/δ_L ~150

ID = 4.5km !!